February 2024
Thesis for Master Degree

Ginsenoside compound K induces PARP-1 hyperactivation promoted by p62-mediated Sirt6 degradation in non-small cell lung cancer cells

Graduate School of Chosun University

Department of Biomedical Sciences

Seok-Woo Hyeong

Ginsenoside compound K induces PARP-1 hyperactivation promoted by p62-mediated Sirt6 degradation in non-small cell lung cancer cells

진세노사이드 compound K의 비소세포폐암 세포에서 p62 의존성 Sirt6 분해에 의한 PARP-1 과활성화 유도에 관한 연구

February 23. 2024

Graduate School of Chosun University

Department of Biomedical Sciences

Seok-Woo Hyeong

Ginsenoside compound K induces PARP-1 hyperactivation promoted by p62-mediated Sirt6 degradation in non-small cell lung cancer cells

Advisor: Prof. Seon-Hee Oh

A thesis submitted to the Graduate School of the Chosun University in partial fulfillment of the requirement for the Master of Science

October 2023

Graduate School of Chosun University

Department of Biomedical Sciences

Seok-Woo Hyeong

Seok-Woo Hyeong's master thesis
has approved by

Chairman Cheol-Hee Choi _____

Committee Member Sung-Hwan Ki _____

Committee Member Seon-Hee Oh _____

December 2023

Graduate School for Chosun University

CONTENTS

LIST OF FIGURES ---------- iii

ABSTRACT(Korean)---------- iv

ABBREVIATIONS ---------- vi

1. **INTRODUCTION** ---------- 1
2. **MATERIALS AND METHODS** ---------- 4
   - 2.1. Reagents and antibodies ---------- 4
   - 2.2. Cell culture ---------- 4
   - 2.3. MTT assay ---------- 4
   - 2.4. Western blot analysis ---------- 5
   - 2.5. RNA interference and overexpression ---------- 5
   - 2.6. Immunoblotting and immunoprecipitation (IP) --------- 6
   - 2.7. Immunofluorescence (IF) ---------- 6
   - 2.8. Subcellular fractionation ---------- 7
   - 2.9. Statistical analysis ---------- 7
3. **RESULTS** ---------- 8
   - 3.1. Morphological changes and proliferation inhibition by CK treatment ---------- 8
   - 3.2. CK induces PARP-1 activation-mediated parthanatos -- 13

3.3. Differenial regulation of CK-induced PARylation and Sirt6 function ---------- 19
3.4. Sirt6 regulates biological functions of PARP-1 ---------- 25
3.5. Sirt6 protein level is regulated by oxidative stress --------- 30
3.6. Subcellular localization of Sirt6 and p62 in response to CK ---------- 38
3.7. Sirt6 interacts with p62 in response to CK ---------- 42
4. DISCUSSION ---------- 46
5. REFERENCES ---------- 51

LIST OF FIGURES

Figure 1. CK-induced morphological changes and various signaling pathways. ---------- 9-12

Figure 2. CK induces PARP-1 activation-mediated parthanatos. ---------- 15-18

Figure 3. CK differentially regulates PARP-1 activation and Sirt6 function. ---------- 21-24

Figure 4. Sirt6 negatively regulates CK-induced PARP-1 activation. ---------- 26-29

Figure 5. CK-induced oxidative stress regulates Sirt6 protein stability. ---------- 32-37

Figure 6. Subcellular translocation of Sirt6 depends on p62. ----- 39-41

Figure 7. Sirt6 interacts with p62 through ubiquitination. ------- 43-45

초록

진세노사이드 Compound K의 비소세포폐암 세포에서 p62 의존성 Sirt6 분해에 의한 PARP-1 과활성화 유도에 관한 연구

형석우
지도교수 : 오 선희 교수
조선대학교 의과학과
조선대학교 대학원

진세노사이드 화합물 K (compound K)는 다양한 암 유형에 대해 항암 효과가 있는 것으로 보고 되었다. 그러나 폐암에서는 분자 메커니즘이 명확하게 정의되어 있지 않았다. 본 연구는 CK가 PARP-1 과활성화 의존성 parthanatos를 유도하고 이는 p62 의존성 히스톤 디아세틸라아제 Sirt6의 단백질 감소에 의해 촉진된다는 것을 규명하였다. CK는 용량 의존적으로 세포 성장을 억제할 뿐 아니라 세포질 내 액포를 형성함으로써 결국 세포사를 유도했다. CK 처리는 procaspase-8의 단백질 수준을 감소시켰으나, procaspase-3 및 PARP-1에 영향을 주지 않았다. 또한, CK 처리는 세포주기 정지 관련 단백질인 p21, p27 및 phospho-p53을 증가시켰다. 자가포식 마커인 LC3-II는 CK 농도 및 배양시간 의존적으로 증가했지만, 자가포식 수용체인 p62는 현저한 감소를 보이지 않았다. 그러나, p62와 LC3-II 수준이 자가포식 억제제에 의해 증가됨으로써, p62가 CK 유도 자가포식에 관여한다는 것을 나타낸다. CK는 PARP-1의 과활성화를 유도하여 parthanatos의 전형적인 특징인

폴리ADP-리보스(PAR)와 세포사멸 유도 인자(AIF)의 세포내 전위 및 염색질 절단을 유도했다. CK처리 후 Sirt6 단백질 수준은 용량 및 시간 의존적으로 감소했으며, 이는 PARP-1 활성화와 반비례 관계를 보여주었다. PAR 수준은 NAD+ 및 Sirt6 과발현에 의해 감소한 반면 Sirt6 녹다운 및 자가포식에 의해 증가하였다. Sirt6 단백질은 PARP-1 억제 및 p62 녹다운에 의해 증가하였다. 면역 형광 염색 및 분획 연구에 의해 Sirt6는 세포질로 이동된 후 p62와 함께 국소화됨을 나타냈으며, 면역 침강법에 의해 Sirt6와 p62 사이의 결합을 확인하였다. 본 연구결과는 p62 의존성 Sirt6 단백질 감소는 PARP-1의 과활성화를 유도하고, 이는 CK 유도 Pathanatos를 증가시킨다는 것을 규명하였다. 따라서 PARP-1 과활성화에 의해 유도된 parthanatos는 CK 유발 암세포 사멸에 중요한 역할을 할 수 있다.

ABBREVIATIONS

CK, compound K

PAR, polyADP-ribose

AIF, apoptosis-inducing factor

Sirt6, silent information regulator 6

NAD+, nicotinamide adenine dinucleotide

ER, endoplasmic reticulum

PARP-1, poly-ADP ribose polymerase 1

PARylation, polyADP-ribosylation

NSCLC, non-small cell lung cancer

BaF1, bafilomycin A1

CQ, chloroquine

ROS, reactive oxygen species

ANI, 4-amino-1,8-naphthalimide

HDAC1, histone deacetylase 1

H3K9Ac, histone H3 lysine 9

MIBG, meta-iodobenzylguanidine

HO-1, heme-oxygenase 1

SOD2, superoxide dismutase 2

MMP, mitochondrial membrane potential

NAC, N-acetyl cysteine

Toco, tocopherol

LMB, leptomycin B

IF, Immunofluorescence

1. INTRODUCTION

Lung cancer is the second most prevalent cancer worldwide and causes the highest number of cancer-related deaths in both men and women. More seriously, the incidence and mortality of lung cancer continues to increase. Causes of increased lung cancer include smoking, air pollution, asbestos, radon, and arsenic. In this situation, many potential chemopreventive agents, including selenium, have been reported to reduce the risk of lung cancer, but no agent has yet shown effective results in the clinical treatment of lung cancer. Therefore, detailed research on the signals that cause lung cancer is required to develop or find effective treatments.

Silent information regulator 6 (Sirt6) is classified as a class III histone deacetylases (Sirt1 to 7) and functions as nicotinamide adenine dinucleotide (NAD^+)- dependent deacetylase and mono-ADP ribosyltransferase (Liszt et al., 2005). Sirt6 exclusively localized in the nucleus (Sharma et al., 2023), reflecting a role for Sirt6 in genomic maintenance, which plays critical roles in various biological processes including aging, cell death and tumorigenesis (Mostoslavsky et al., 2006; Houtkooper et al., 2012). Upon stress, Sirt6 translocate to the cytoplasm and involves in stress granule formation, promoting cell survival (Campos-Melo, et al., 2021; Jedrusik-Bode et al., 2013). It has been reported that Sirt6, localized in the endoplasmic reticulum (ER), can regulate inflammation through tumor necrosis factor-α secretion (Jiang et al., 2013; Bresque et al., 2022). There are also conflicting reports that Sirt6 functions as a tumor promoter or suppressor for cancer. Sirt6 downregulated in some cancers, including hepatocellular carcinoma (Marquardt, et al., 2013), colorectal cancer (Liu et al., 2018), and head and neck squamous cell carcinoma (Park et al., 2021), and that was associated with apoptosis suppression. Whereas, in breast cancer cells, Sirt6 overexpression enhanced resistance to anticancer drugs, such as paclitaxel and epirubicin (Khongkow et al., 2013). Various types of lung cancer cells, including NCI-H460 and A549, and prostate cancer cells, expressed high levels of Sirt6, and knockdown of Sirt6 induced apoptosis (Liu et al., 2013; Krishnamoorthy and Vilwanathan, 2020). These contrasting results of Sirt6 suggest that it may be due to cell type-specificity as well as the diverse functions of Sirt6. Therefore, further studies of its molecular mechanisms are required to

elucidate the role of Sirt6 in various pathological conditions.

Poly (ADP-ribose) polymerases (PARPs) play an important role in various cellular processes, including DNA repair, transcription, replication, chromatin remodeling (Morales et al., 2014). PARP-1 is the best known of the PARP family, and plays an important role in DNA repair associated with cell survival. Upon DNA damage, PARP-1 promotes the transfer of ADP-ribose units from NAD+ to itself or to other proteins such as histone and non-histone proteins, and post-translational modifications of PARP-1 play an important role in DNA damage repair (Bae et al., 2012). However, massive DNA damage results in PARP-1 overactivation via polyADP-ribosylation (PARylation), reducing cellular ATP levels and eventually leading to parthanatos cell death (Andrabi et al., 2006). In addition, upon severe DNA damage, PARP-1 is cleaved by caspases 3 and 7, to two enzymatically inactive fragments (89 and 24 kDa) and inducing apoptosis (D'Amours et al., 2001). Sirt6 promotes DNA repair via catalizing ADP-ribosylation of PARP-1 (Mao et al., 2011). In this context, the relationship between Sirt6 and PARP-1 needs to be elucidated to better understand the opposing effects of Sirt6 on cancer cells.

Ginsenoside compound K [CK, 20-*O*-(β-d-glucopyranosyl)-20(*S*)-protopanaxadiol], a main metabolite of protopanaxadiol saponins, has been reported to be anticarcinogenic in various types of cancer cells (Zouh et al., 2021). CK induced endoplasmic reticulum (ER) stress through regulating STAT3 phosphorylation and ER Ca^{2+} release in hepatocellular carcinoma cells (Zhang et al., 2018) and human lung adenocarcinoma A549 and human lung squamous cell carcinoma SK-MES-1 (Shin et al., 2018). ROS have been shown to play an important role in CK-induced apoptosis through mitochondrial- and caspase dependent-signaling pathways in HT-29 human colon cancer cells and HL-60 human leukemia cells. (Lee et al., 2010; Cho et al., 2009). Furthermore, CK induced autophagy and apoptosis via AMPK-mTOR and JNK signaling pathways in A549 and H1975 cells (Li et al., 2019). However, much remains to be elucidated about the molecular mechanism of the role of CK in antitumor effects. Recently, ginsenoside Rc was reported as a Sirt6 activator that prevents non-alcoholic fatty liver disease by increasing deacetylase activity (Yang et al., 2020). In palmitate-treated podocytes, ginsenoside Rb3 reduced

apoptosis and inflammation via upregulation of Sirt6 and PPARδ (Oh et al., 2022). Additionally, in patients with non-small cell lung cancer (NSCLC), high cytoplasmic expression of Sirt6 was associated with poor prognosis and decreasing chemosensitivity (Azuma et al., 2015). Although previous studies have been demonstrated that CK induces apoptosis in lung cancer cells, however, there is no reports demonstrating an involvement of Sirt6 in CK-induced apoptosis. Therefore, to better understand the chemopreventive effect of CK, more studies related with cytotoxic mechanism are required.

Therefore, in this study, we explored the involvement of Sirt6 and PARP-1in the anti-cancer effect of ginsenoside CK in non-small cell lung cancer H460 cells overexpressing Sirt6. Our study showed that the anticancer effect of CK is involved in PARP-1 activation-mediated parthanatos promoted by p62-mediated Sirt6 degradation.

2. MATERIALS AND METHODS

2.1. Reagents and antibodies

Compound K, 3-(4,5-dimethylthiazol-2-yl)-2,5-diphenyltetrazolium bromide (MTT), Hoechst 33342, bafilomycin A1, and anti-β-actin antibody were obtained from Sigma (St, Louis, MO). p21, rhodamine-conjugated goat anti-rabbit, and FITC-conjugated goat anti-mouse antibodies were purchased from Santa Cruz Biotechnology (Dallas, TX, USA). PARP-1, procaspase-3, phospho-p53 (S15), LC3B, p27, and p21antibodies were purchased from Cell Signaling Technology (Beverly, MA, USA). SQSTM1/p62 antibody was purchased from Abnova (Taipei city, Taiwan).

2.2. Cell culture

H460 human lung cancer cells (HTB-177 ™) were obtained from the American Type Culture Collection (Rockville, MD, USA, ATCC). The cell lines were maintained in Dulbecco's modified Eagle's medium (WelGene, Gyeongsan, Republic of Korea) supplemented with 10% fetal bovine serum (WelGene) and penicillin-streptomycin (WelGene). The cells were cultured at 37°C in a humidified incubator with 5% CO_2.

2.3. MTT assay

H460 cells were suspended in complete media, at a concentration of 1 x 10^5 cells / ml, and samples (200 μl) of the cell suspensions were seeded onto 48-well plates and cultured overnight. Cells were then exposed to chemicals for 24 hr. After 4 h of incubation with MTT (0.5 mg / ml), and the formazan crystals were dissolved with DMSO. Absorbances were measured at 540 nm using an ELISA microplate reader (Perkin-Elmer).

2.4. Western blot analysis

Proteins were extracted from the collected pellet using lysis buffer (1 % Triton X-100, 150 nM NaCl, 5 mM EDTA and protease inhibitors), quantified using BCA Protein Assay Kit (USA) and the concentration was measured at 595 nm using a Microplate reader. 20-50 μg of protein was electrophoresed using 10-12 % SDS-PAGE gel and transferred to PVDF membrane. In order to inhibit the binding of nonspecific proteins, membranes of 5 % skim milk made in TBS (20 mmol / L Tris, 137 mmol / L NaCl, pH7.6). Primary antibodies were reacted overnight at 4℃. The membrane was washed three times with TBST solution containing 0.05 %. The secondary antibody was reacted at room temperature for 2 hr. Finally, the membrane was identified as a Super HR-A (Fuji film, Japan) component of the Fuji Medical X-RAY membrane using a Millipore immobilon Western chemiluminescent HRP substrate.

2.5. RNA interference and overexpression

Target-specific siRNAs for Atg5 (5'-GAGUCAGCUAUUUGACGUU-3') and p62 (5'-CUU GUA GUU GCA UCA CGU A-3') were synthesized by Genolution (Seoul, Korea). Cells were seeded into 6-well plates and transfected with 20 pM siRNA or scrambled siRNA (Thermo Fisher Scientific) using Lipofectamine™ RNAiMAX reagent (Invitrogen). pcDNA3.1-Sirt6 was kindly provided by Dr. Park Byung-Hyun (Chonbuk National Univ.). Plasmid DNA (0.5 μg) and empty vector were transfected into cells using X-tremeGENE HP-DNA transfection reagent (Roche) according to the supplier's protocol. Media was replaced with fresh and complete media after 6 hr. Cells were incubated for an additional 1-2 d before further treatment.

2.6. Immunoblotting and immunoprecipitation (IP)

Cells were lysed in lysis buffer containing protease cocktails (Roche). Proteins (15 – 35 μg) were resolved using 10% – 12% SDS-PAGE, and transferred to polyvinylidene difluoride (PVDF) membranes (Millipore), blocked with 5% skim milk (Bioshop), and then probed with primary and secondary antibodies. Proteins were visualized using a chemiluminescent substrate (Millipore). For IP, cells were lysed in lysis buffer [0.05 M Tris-HCl (pH 7.4), 250 mM NaCl, 0.25% Triton X-100, 10% glycerol] with protease cocktails. Total proteins (800 μg) were precleared using 50% protein G Plus-agarose beads (Santa Cruz) and centrifuged at 12,000 × g for 10 min at 4°C. The supernatants were incubated with the indicated primary antibody, rabbit IgG (Sigma-Aldrich), or mouse IgG (Sigma-Aldrich) overnight at 4°C. The immunocomplexes were captured using protein G Plus-agarose beads and washed with ice-cold PBS several times. The washed beads were resuspended in 2X-Laemmli loading buffer, boiled, and then the proteins were eluted and processed for immunoblotting.

.

2.7. Immunofluorescence (IF)

After culturing cells on a cover slip (Marienfeld), they were fixed in neutral-buffered formalin (NBF, Sigma-Aldrich) for 10 min on ice. The cells were then washed with PBS and treated with 0.05% Triton X-100 (Sigma) for 20 min. After washing with PBS, the cells were blocked with 2% bovine serum albumin (Bioshop). The cells were then incubated with primary antibodies and fluorescently conjugated secondary antibodies. Nuclei were counterstained with Hoechst 33342 (1 μg/mL), and images were captured using a Nikon Eclipse TE300 fluorescence microscope.

2.8. Subcellular fractionation

Cells were washed with PBS, resuspended in hypotonic buffer [20 mM HEPES-KOH, pH 7.0, 10 mM KCl, 1.5 mM $MgCl_2$, 1 mM sodium EDTA, 1 mM EGTA, 250 mM sucrose (Sigma-Aldrich] supplemented with cOmplete Mini EDTA-free protease inhibitor mixture tablets (Roche Applied Science). The cells were homogenized by passing them through a needle, and then centrifuged at 800 g for 4 min. The pellet was the nuclei-rich insoluble fraction. The supernatant containing the organelles and cytosol was then centrifuged for 20 min at 10,000 × *g* at 4°C. The new supernatant and cytoplasmic organelle-rich pellet were used as the soluble and particulate fractions, respectively.

2.9. Statistical analysis

All experiments were repeated at least three times, and values are expressed as means ± standard deviation (SD). Statistical analysis was performed using Student's *t*-test, or one-way ANOVA.). A value of $p < 0.05$ was considered statistically significant.

3. RESULTS

3.1 Morphological changes and proliferation inhibition by CK treatment

We examined morphological changes induced by varying concentrations of CK. CK treatment induced a formation of cytoplasmic vacuoles, which began as early as 3h of treatment, and continuously increased in the number and size, and finally, detached from the culture dish (Fig. 1A). To elucidate the sensitivity of H460 cells to CK, cells were exposed to various concentrations of CK for 24 h and analyzed using an MTT assay. The half-maximal inhibitory concentration (IC_{50}) of CK was approximately 37 ug/ml (Fig. 1B). To elucidate the signaling pathways involved in the sensitivity to CK at the biochemical level, we first investigated the expression of apoptosis-related proteins. H460 cells induced decreasing caspase-8, but not of caspase-3. Furthermore, the level of the 116 kDa poly-ADP ribose polymerase 1 (PARP-1) protein was markedly reduced at high concentrations (40 and 50 μg/ml), however, no significant apoptotic cleavage of PARP-1. Next, we determined whether cell cycle process is involves in CK-induced growth inhibition, and we found that upregulating p27, p21, and phosphor (p)-p53, indicating that CK induces DNA damage-mediated cell cycle arrest (Fig. 1C). In addition, CK treatment dose- and time-dependently increased the autophagy marker LC3-II. However, the autophagy adapter p62 did not correlate with LC3-II induction (Fig. 1D). Together, these results indicate that CK-induced cellular damage is implicated with various signaling pathways, including caspase-independent cell death pathway, cell cycle arrest, and autophagy.

Figure 1A

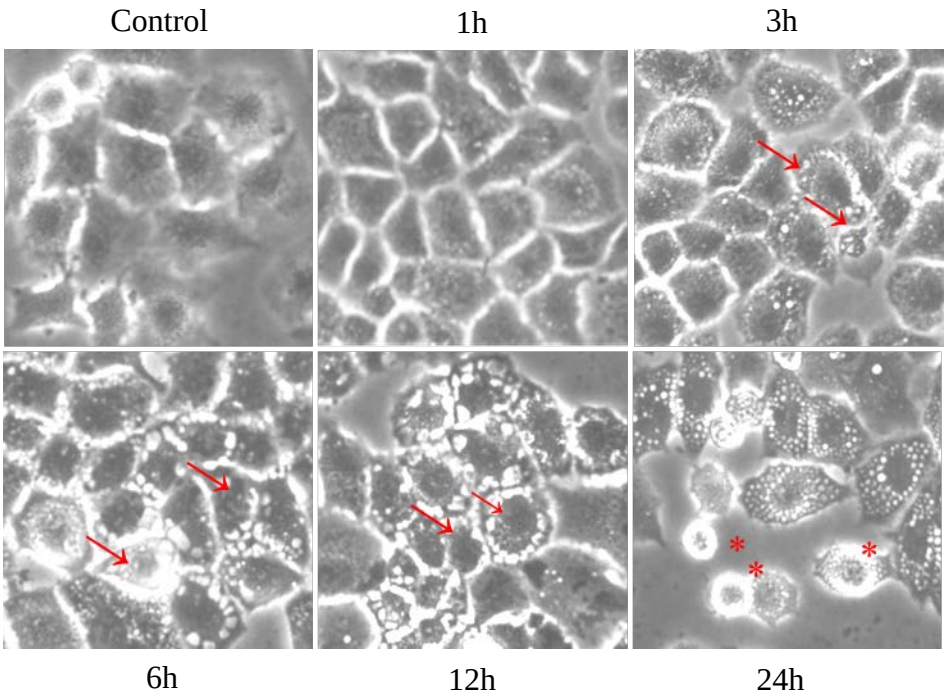

Figure 1A. H460 cells were treated with increasing concentrations of CK for up to 24 hr, and the morphological changes were observed using phase-contrast microscopy.

Figure 1B

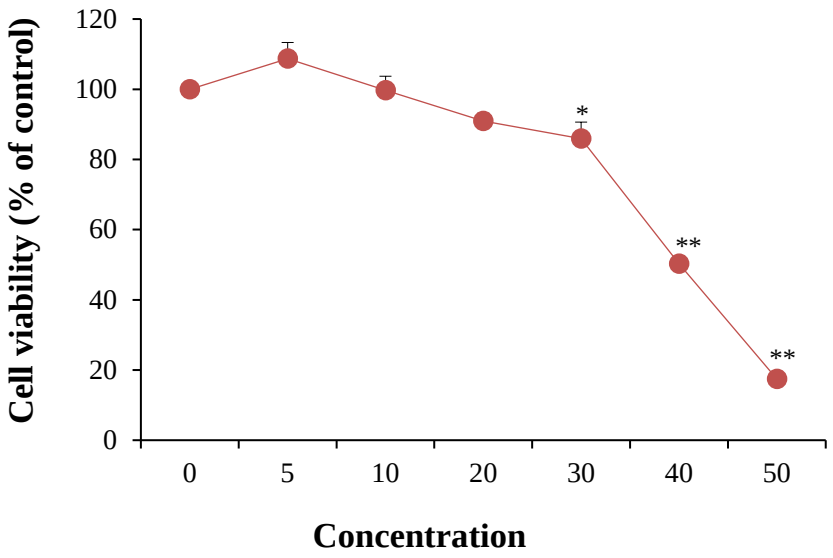

Figure 1B. H460 cells were exposed to increasing concentrations of CK for 24 hr, and their viability was determined using an MTT assay. Data are expressed as the mean ± SD of the fold-increase compared to the untreated control from three independent experiments performed in triplicate. $^{*}P < 0.05$; $^{**}P < 0.005$.

Figure 1C

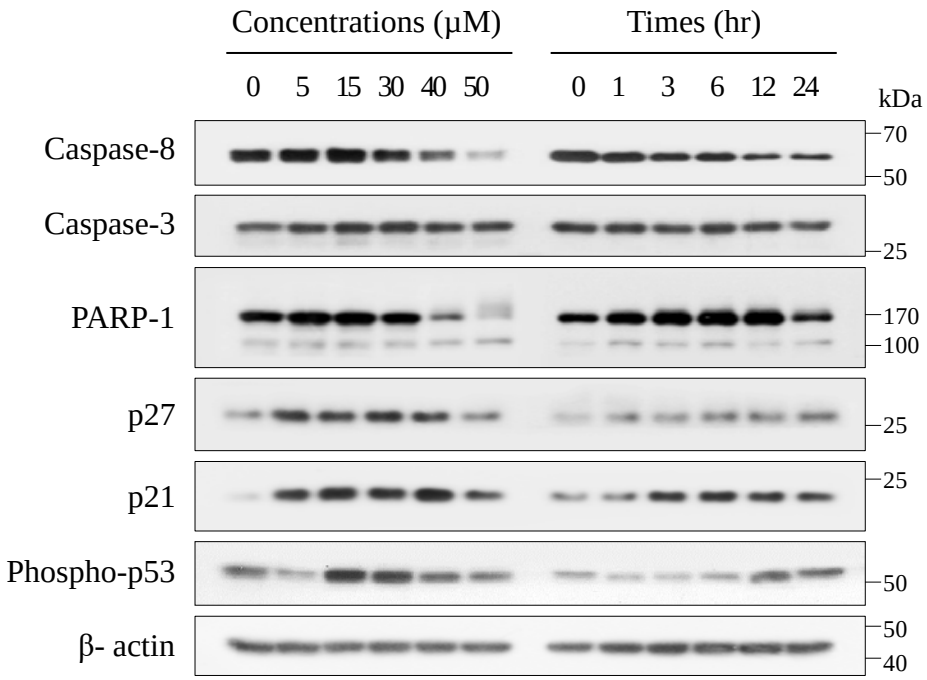

Figure 1C. H460 cells exposed to increasing concentrations of CK for 18 hr and incubated for up to 24 hr with 35 μg/ml CK, harvested, and lysed. The expression levels of the indicated proteins were assessed using immunoblotting. β-actin was used as the loading control. Data shown are based on three separate experiments.

Figure 1D

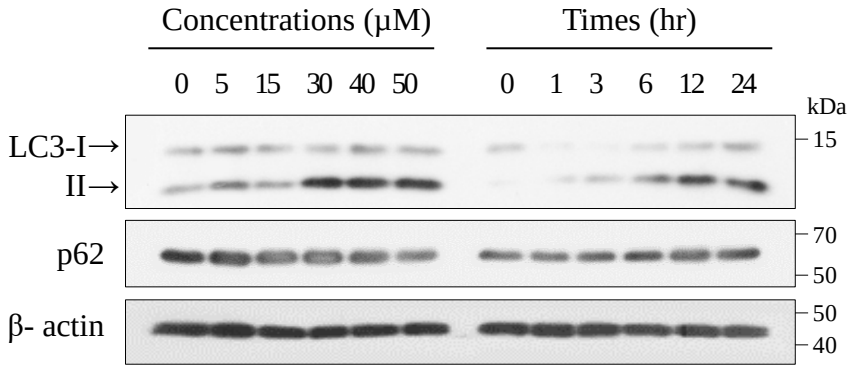

Figure 1D. H460 cells were exposed to increasing concentrations of CK for 18 hr and incubated for up to 24 hr with 35 μg/ml CK, harvested, and lysed. The expression levels of the indicated proteins were assessed using immunoblotting. β-actin was used as the loading control. Data shown are based on three separate experiments.

3.2. CK induces PARP-1 activation-mediated parthanatos

Despite of cell growth inhibition, CK exposure did not induce significant apoptotic cleavage of PARP-1 and caspase-3. We thus examined PARP-1 activation by specific antibody for polyADP-ribose (PAR). PAR accumulated in a dose- and incubation time-dependent manner, beginning to be induced at 3 hr and increasing significantly at 12 hr in time-dependent experiments using 35 ug/ml CK. This indicates that polyADP-ribosylation (PARylation) may be involved in CK-induced cell death (Fig. 2A). To confirm whether CK-induced PARylation was induced by post-translational modification of PARP-1, PARP activity was inhibited by 3-amino benzamide (AB) and 4-amino-1,8-naphthalimide (ANI), and a pancaspase inhibitor zVAD-fmk. CK-induced PARylation almost completely suppressed by ANI and 3-AB and partially zVAD-fmk. PARP inhibition generated in apoptotic cleavage fragment, 89 kDa, and further decreased caspase-8 and caspase-3 protein levels compared to CK-treated cells, which was inhibited by zVAD-fmk (Fig. 2B). These results indicate that CK can modulate the biological functions of PARP-1 in a context-dependent manner.

Overactivation of PARP-1 leads to cell death, refer to parthanatos. To elucidate whether the hyper-PARylation induced by CK treatment caused for parthanatos, we first observed the morphological changes occurring after CK treatment. Chromatin shrinkage and a distinct chromatin fragmentation arranged in rings along the nuclear membrane (arrows) were observed in CK-treated cells. These are typical features of parthanatotic cell death, different from the apoptotic nuclear changes, such as nuclear condensation and fragmentation (Fig. 2C). To further evidence for parthanatos, we performed subcellular fractionation studies. CK-treated cells were fractionationed into insoluble (i.e. nuclei-rich membranes), soluble (i.e. cytosol), and particulate (i.e. mitochondria) fractions. The purities of the fractions were confirmed by immunoblotting for specific protein markers, such as histone deacetylase 1 (HDAC1), SOD2, and β-actin for nuclear, mitochondria, and cytosolic compartments, respectively. After CK treatment, the PAR polymer mainly localized in the cytosolic compartment and to the lesser extent, insoluble and particulate fractions. Apoptosis inducing factor (AIF) decreased gradually in the particulate fractions and

upregulated in the nucleus-rich insoluble fractions (Fig. 2D). These results evidenced that CK-induced cellular damage is associated with PARP-1 activation-mediated parthanatos.

Figure 2A

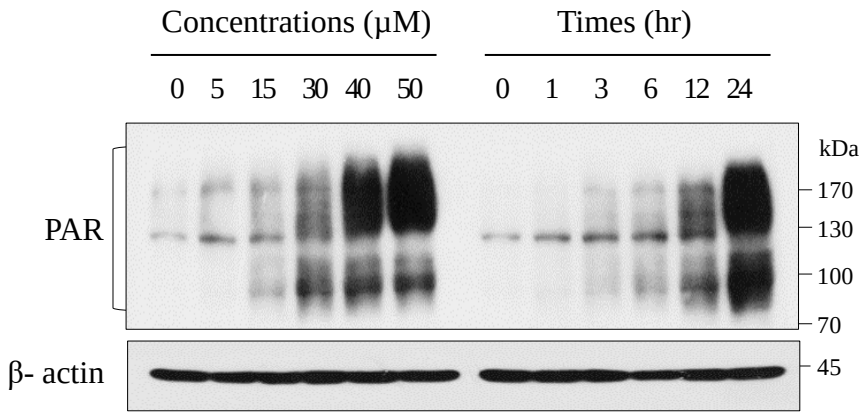

Figure 2A. CK induces PARP-1 hyperactivation. H460 cells were treated with increasing concentrations of CK and incubated for up to 24 hr, harvested, and lysed. PAR expression levels were assessed by using polyADP-ribose antibody by immunoblotting. β-actin was used as the loading control. Data shown are based on three separate experiments.

Figure 2B

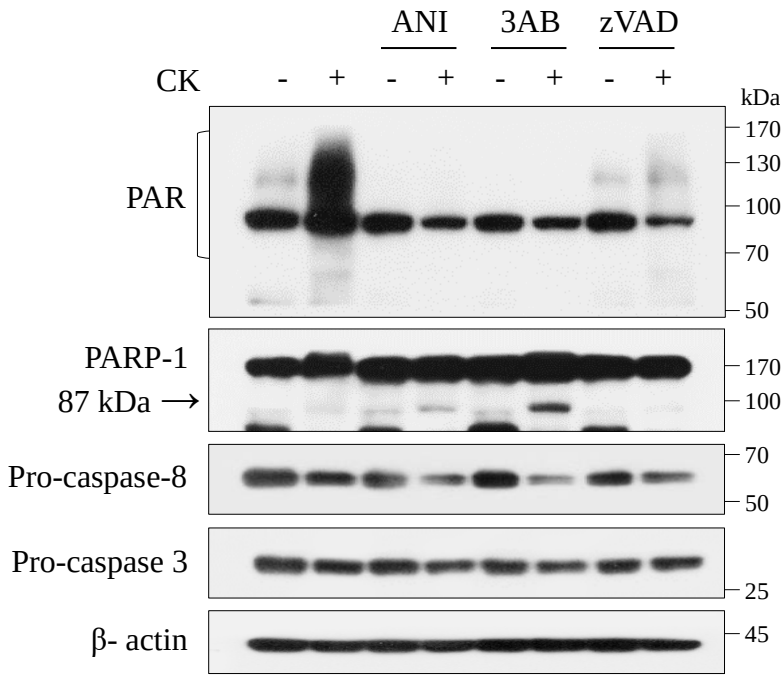

Figure 2B. Inhibition of PARP-1 induces apoptotic PARP-1 cleavage. H460 cells were pretreated with 3-AB, ANI, zVAD-fmk and DMSO control for 2 hr, and continuously exposed to CK (35 μg/ml) for 18 hr, harvested, and lysed, and the levels of the indicated proteins in the lysates were analyzed using immunoblotting. β-actin was used as the loading control.

Figure 2C

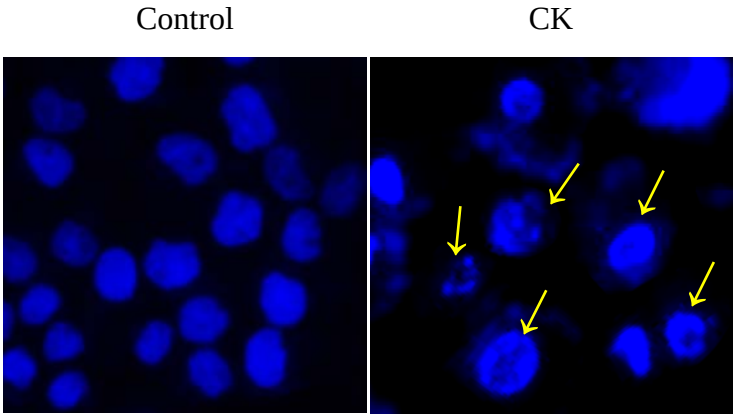

Figure 2C. CK induces parthanatos. Nuclear changes in CK-exposed H460 cells. H460 cells cultured on coverslips were treated with CK for 18 hr. Cells were fixed and Nuclei were stained with Hoechst 33342, and images were acquired using a fluorescence microscope (Nikon, Eclipse TE300) (200x).

Figure 2D

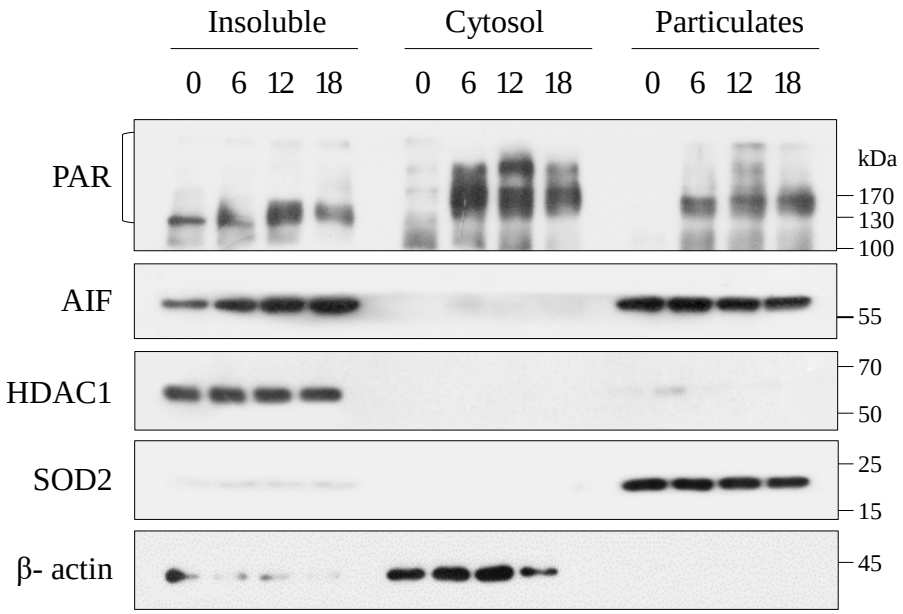

Figure 2D. H460 cells were exposed to CK for 6, 12, and 18 hr and subjected to subcellular fractionation into nuclear-enriched, cytosol, and mitochondria-edriched fractions. The purity of each fractions was determined using immunoblotting for HDAC1, β-actin, and SOD2, respectively. Data are representative of n > 3.

3.3. Differential regulation of CK-induced PARylation and Sirt6 function

Sirt6 has a dual function as both monoADP-ribosyl transferase and NAD^+-dependent deacetylase of histone H3 (Choi and Mostoslavsky, 2014). In addition, Sirt6 can stimulate PARP-1 activity via monoADP-ribosylation (Mao et al., 2011). Therefore, we investigated that the role of Sirt6 in CK-induced PARP-1 activation. To elucidate this, we first examined Sirt6 protein level in CK-exposed cells. H460 cells expressed high basal level of Sirt6, and it decreased by high concentrations of CK (≥30 μg/ml) and after 12 h of incubation time gradually decreased. The deacetylase effect of Sirt6 was analyzed by the level of histone H3 lysine 9 (H3K9Ac). The decreasing of Sirt6 level led to upregulate H3K9Ac, indicating that CK inhibits deacetylase activity of Sirt6 at lysine 9 via decreasing Sirt6 protein (Fig. 3A). In addition, the Sirt6 expression level showed an inverse correlation with the CK-induced PAR accumulation (Fig. 2A). We thus examined whether the monoADP-ribosylase activity of Sirt6 plays a role to PARP activation induced by CK, H460 cells were treated with the monoADP-ribosylation inhibitor meta-iodobenzylguanidine (MIBG) (Smets et al., 1990), and the results obtained were compared with those of the polyADP-ribose polymerase inhibitor 3-AB. 3-AB treatment completely inhibited CK-induced PAR accumulation and up-regulated Sirt6 and down-regulated its downstream H3K9Ac. MIBG treatment partially reduced CK-induced PAR accumulation and further reduced CK-induced Sirt6 protein levels, increasing H3K9Ac (Fig. 3B), indicating that CK can regulate both functions of Sirt6.

Since Sirt6 function and PARP activation are depend on nicotinamide adenine dinucleotide (NAD+) level (Liu et al., 2018), we investigated the effect of exogenous NAD+ supply on CK-induced Sirt6 and PARylation. NAD+ supplement markedly suppressed CK-induced PAR accumulation, upregulated Sirt6 protein and downregulated H3K9Ac, suggesting that CK-induced PARylation was not depend on exogenous NAD+ levels, but the deacetylase activity of Sirt6 is dependent on NAD levels. We determined the effects of PARylation and Sirt6 expression on cell viability using MTT assay. NAD+ treatment significantly increased but did not completely recovered CK-induced cell viability (Fig. 3C, D), indicating that CK can trigger

multiple cell death pathways. This suggests that PARP1 activation and Sirt6 function play complementary roles in CK-induced cell growth inhibition.

Figure 3A

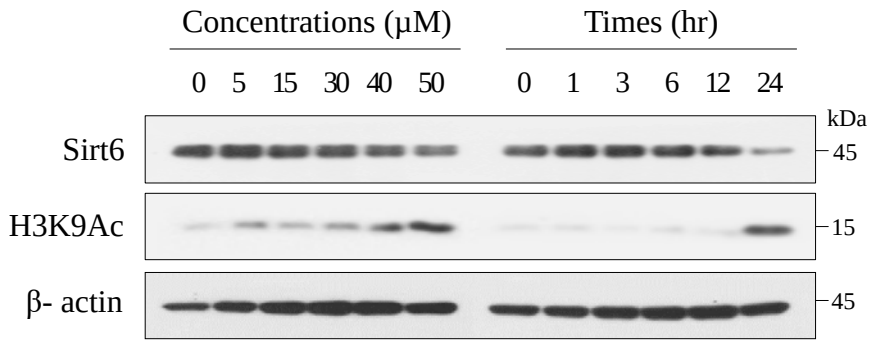

Figure 3A. CK degrades Sirt6 protein. H460 cells were treated with increasing CK concentrations for 18 hr or with 35 μg/ml for up to 24 hr, harvested, and lysed, and the levels of the indicated proteins in the lysates were analyzed using immunoblotting. β-actin was used as the loading control.

Figure 3B

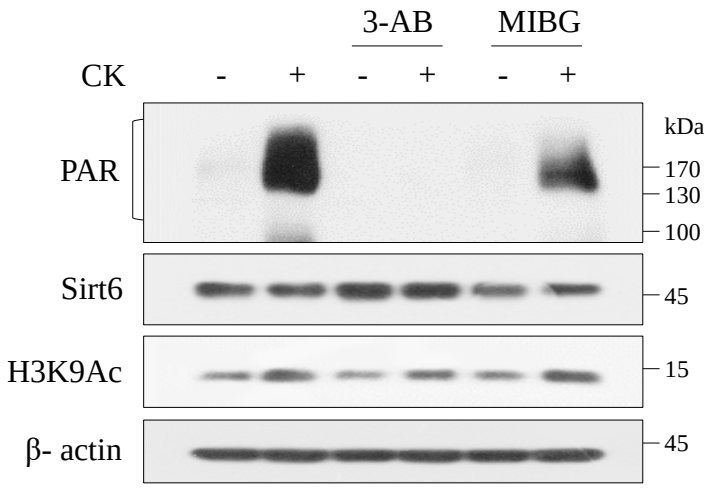

Figure 3B. Inhibition of PARP-1 increases Sirt6 protein. H460 cells were pretreated with 3-AB (5 μM) and MIBG (25 μM) for 2 hr and continuously treated with CK (35 μg/ml) for 18 hr, and the indicated proteins were analyzed by immunoblotting.

Figure 3C

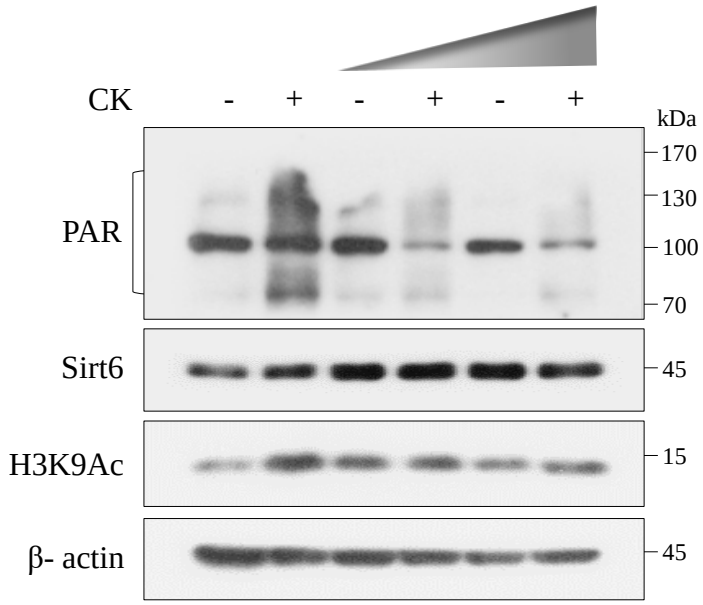

Figure 3C. H460 cells were pretreated with increasing concentrations of NAD+ (25 and 50 nM) and continuously exposed to CK (35 μg/ml) for 18 hr, and the indicated proteins were analyzed by immunoblotting.

Figure 3D

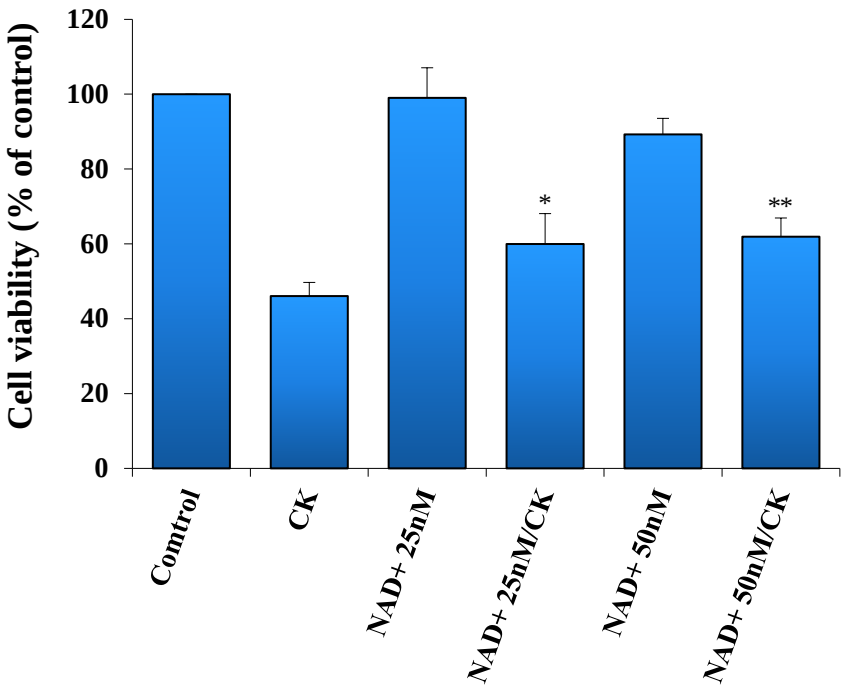

Figure 3D. H460 cells were pretreated with increasing concentrations of NAD+ (25 and 50 nM) and continuously exposed to CK (35 μg/ml) for 18 h, and their viability was determined using an MTT assay. Data are expressed as the mean ± SD of the fold-increase compared to the untreated control from three independent experiments performed in triplicate. * $P < 0.05$; ** $P < 0.005$

3.4. Sirt6 regulates biological functions of PARP-1

In the above series of experiments, we found that PARylation levels in response to CK showed contrary results to Sirt6 protein levels. To investigate the involvement of Sirt6 in PARP-1 function, and *vice versa*, the Sirt6 gene was knocked down by transfection with Sirt6 siRNA, and knockdown efficiency was assayed for the Sirt6 protein by immunoblotting (Fig. 4A). CK treated for 4 and 18 h to Sirt6-knockdowned cells, respectively. At early time when sirt6 protein upregulated by CK treatment, Sirt6 knockdown slightly upregulated PARylation and H3K9Ac, which were markedly enhanced at later time 18 h. Sirt6 knockdown induced PARP-1 cleavage (Fig. 4B). In morphological analysis, CK exposure for 18 h to Sirt6-knockdowned cells massively induced cytoplasmic vacuoles compared to CK-exposed wild type cells (Fig. 4C).

Next, we examined the role of Sirt6 under overexpression condition. The Sirt6 overexpression confirmed at 48 hr after transfection by immunoblotting (Fig. 4D). CK exposure to Sirt6-overexpressing H460 cells markedly reduced CK-induced cytoplasmic vacuoles (Fig. 4E). Sirt6 overexpression reduced CK-induced PARylation and H3K9Ac and did not induce PARP-1 cleavage (Fig. 4F). These results indicate that CK-induced PARylation level is inversely correlated with Sirt6 protein levels. It also shows that Sirt6 protein level can play a critical role in biological functions of PARP-1.

Figure 4A-B

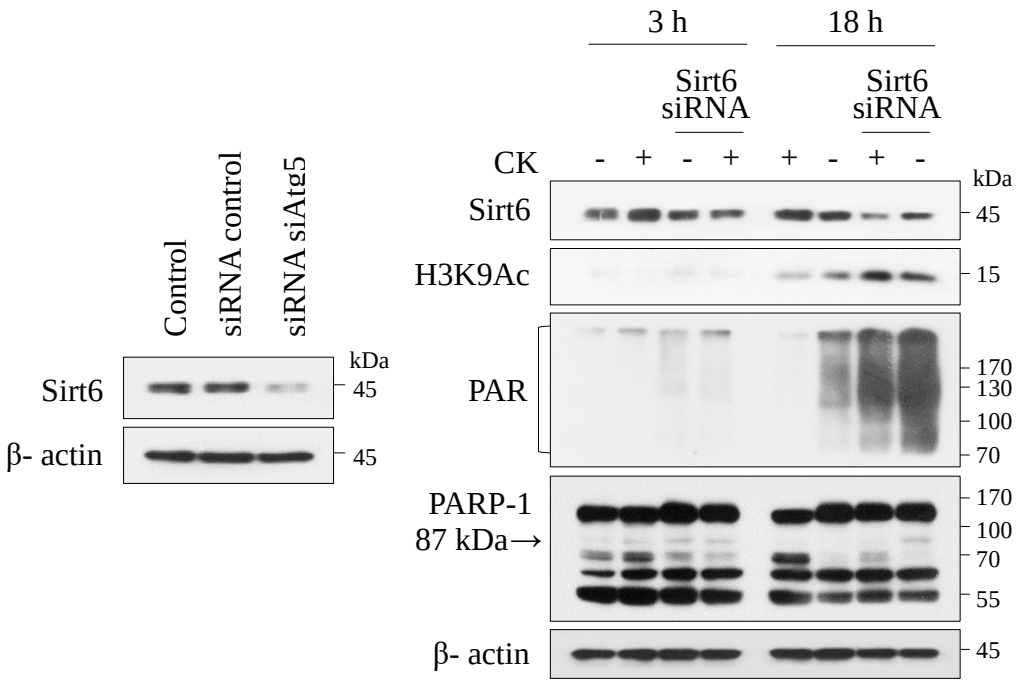

Figure 4A-B. (**A**) Knocked down efficiency for Sirt6-specific siRNA was evaluated using immunoblotting for Sirt6. NC denotes negative control. (**B)** H460 cells silenced with the NC siRNA or Sirt6 siRNA were exposed to CK (35 μg/ml) for 18 hr, and the levels of the indicated proteins in the lysates were analyzed using immunoblotting. β-actin was used as the loading control (n = 3).

Figure 4C

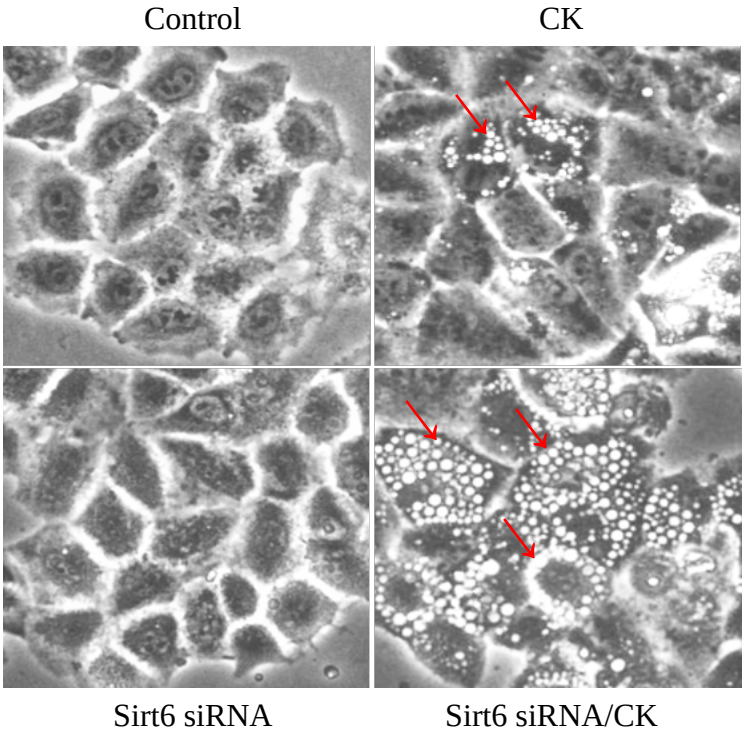

Figure 4C. Morphological changes in CK-exposed Sirt6 knockdowned cells were observed using phase contrast microscopy. Arrows indicate cytoplasmic vacuoles.

Figure 4D-E

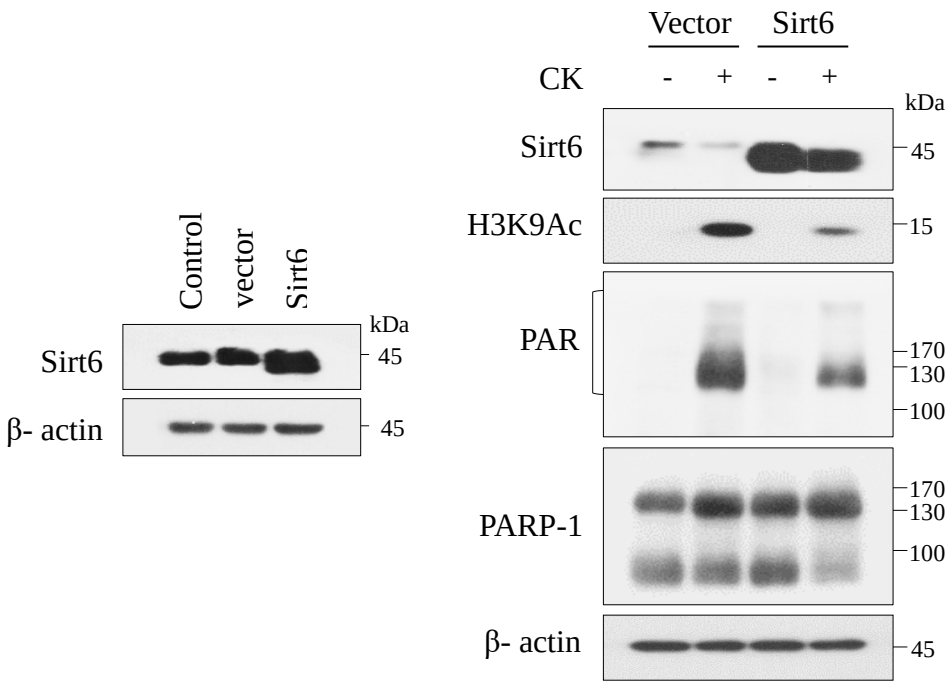

Figure 4D-E. (**D**) Transfection efficiency was evaluated at 24 hr of transfection with empty vector and pcDNA3.1-Sirt6 by immunoblotting. β-actin was used as the loading control. (**E**) H460 cells overexpressing Sirt6 were treated with CK for 18 hr, and the levels of the indicated proteins in the lysates were analyzed using immunoblotting. β-actin was used as the loading control.

Figure 4F

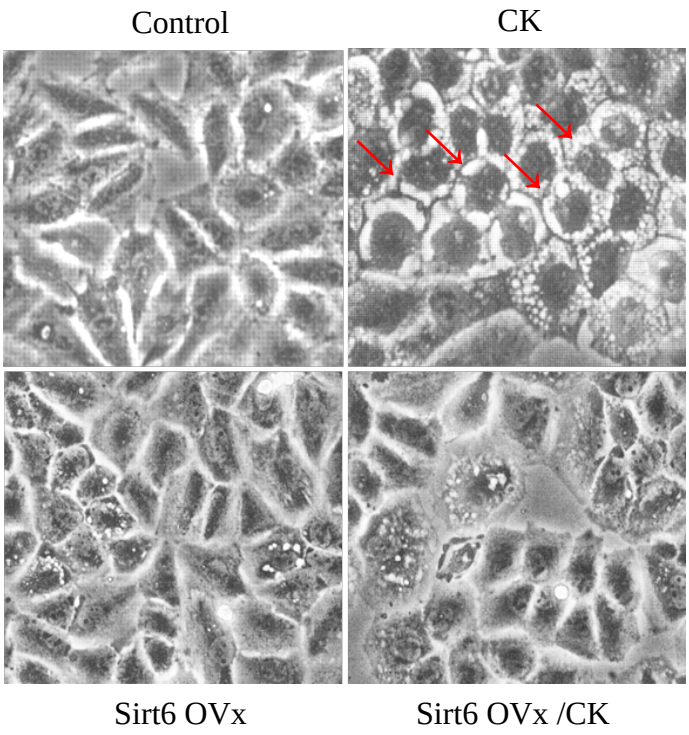

Figure 4F. H460 cells overexpressing Sirt6 were treated with CK for 18 hr, and observed morphological changes

3.5. Sirt6 protein level is regulated by oxidative stress

To further elucidate the role of Sirt6 in CK-induced cellular damage, we examined the molecular mechanisms implicated in regulating of Sirt6 protein. In the present study, Sirt6 protein level decreased by high CK concentrations and later incubation time (≥12 hr) (Fig. 3A). It has been reported that Sirt6 plays a protective role against oxidative stress (Pan et al., 2016). CK treatment induced heme-oxygenase (HO)-1 and upregulated superoxide dismutase (SOD)2 in dose- and time-dependent manner (Fig. 5A), indicating that CK induces oxidative stress. To elucidate whether CK-induced oxidative stress is associated with mitochondrial damage, we examined the changes in the mitochondrial membrane potential (MMP) by staining with JC-1, the selective MMP probe. The control cells exhibited red fluorescence and gradually changed to green fluorescence, and finally, most cells emitted green fluorescence after 8 h of CK exposure, indicating MMP destruction and mitochondrial damage (Fig. 5B). Next, we investigated the relationship between Sirt6 and oxidative stress. To elucidate this, antioxidant enzymes were evaluated in CK-exposed Sirt6-knockdowned cells. Sirt6 knockdowned cells upregulated HO-1 and SOD2 in response to CK (Fig. 5C), while Sirt6 overexpressing cells reduced CK-induced HO-1 and SOD2 (Fig. 5D). To further elucidate these results, cells were treated with antioxidants, including N-acetyl cysteine (NAC) and tocopherol before adding CK. Antioxidant treatment recovered Sirt6 protein levels decreased by CK, decreased HO-1 and SOD2, and also induced a decrease in autophagy and an increase in p62. However, antioxidants upregulated on the CK-induced PARylation level (Fig. 5E). Antioxidant treatment significantly increased CK-induced cell viability but did not completely restore it, probably due to high activation of PARP-1 (Fig. 5F). Collectively, these results indicate that Sirt6 can be used as a marker for CK-induced oxidative stress. Together, these results indicate that Sirt6 is reduced in response to CK-induced oxidative stress.

Antioxidant treatment upregulated CK-induced Sirt6 protein but increased PARylation levels, which was accompanied by decreased autophagy. We thus investigated the involvement of autophagy in CK-induced Sirt6 protein expression and PARylation. Autophagy inhibition by

using chemical inhibitors, including bafilomycin (BaF1) and chloroquine (CQ), accumulated LC3-II and p62, resulting in autophagy inhibition, and further reduced CK-induced Sirt6 protein, increasing SOD2, and HO-1. Additionally, autophagy inhibition increased PAR level (Fig. 5G). These results were further confirmed by genetic knockdown of autophagy gene. Autophagy-related gene *ATG5* knockdown markedly decreased CK-induced LC3-II

Figure 5A

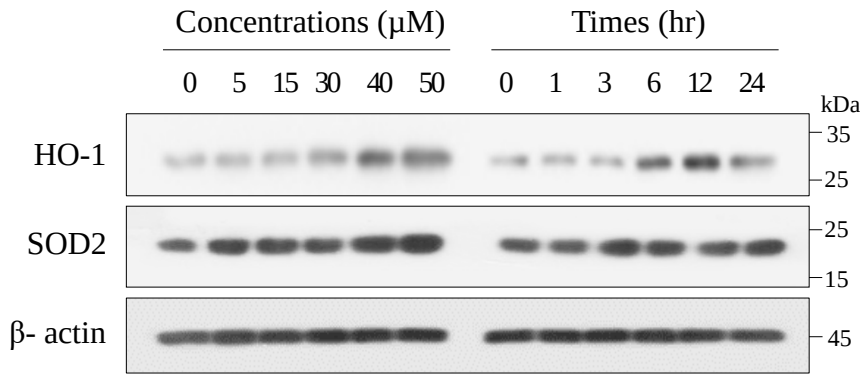

Figure 5A. CK induces oxidative stress. H460 cells were treated with increasing CK concentrations for 18 hr or with 35 μg/ml for up to 24 hr, harvested, and lysed, and the levels of the indicated proteins in the lysates were analyzed using immunoblotting. β-actin was used as the loading control.

Figure 5B

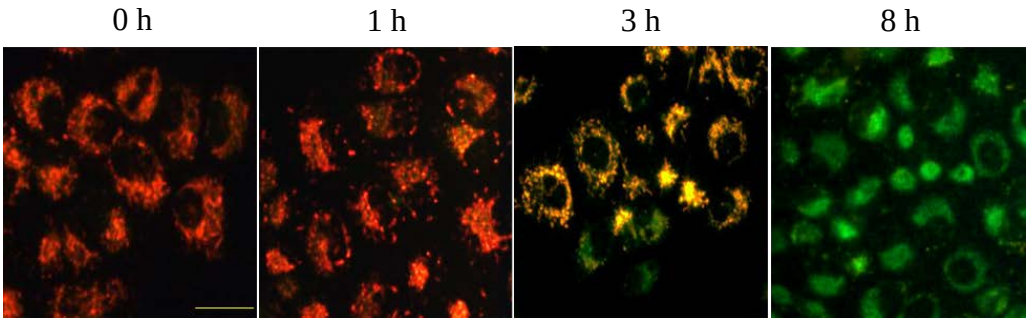

Figure 5B. H460 cells were exposed to CK for up to 8 hr, and stained with JC-1 dye. The images were acquired using a fluorescence microscope. Scale bar = 25 μm.

Figure 5C-D

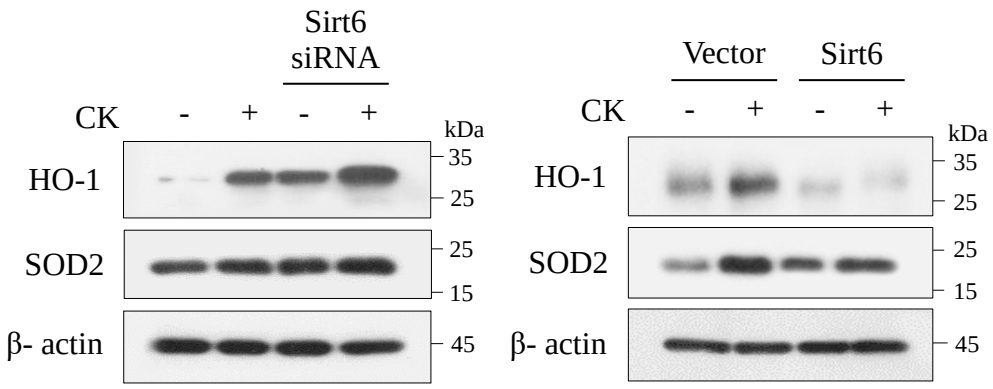

Figure 5C-D. Sirt6 protein regulates CK-induced oxidative stress. H460 cells silenced with the Sirt6 siRNA (**C**) or overexpressed with Sirt6 (**D**) were exposed to CK (35 μg/ml) for 18 hr, and the levels of the indicated proteins in the lysates were analyzed using immunoblotting. β-actin was used as the loading control (n = 3).

Figure 5E

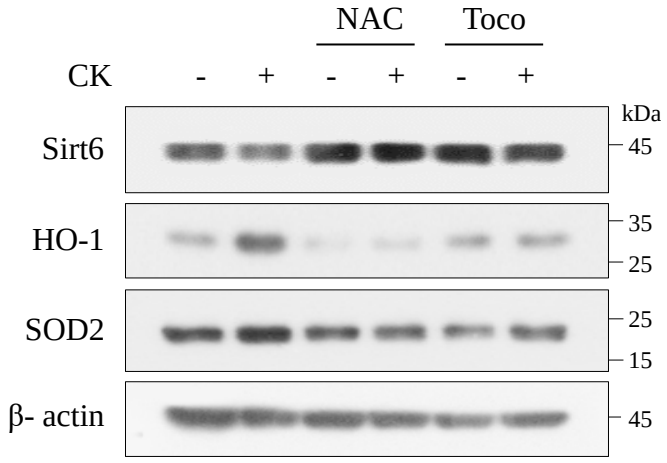

Figure 5E. H460 cells were exposed to CK (35 μg/ml) for 18 hr after pretreatment with NAC (5 mM) and tocopherol (Toco, 25 μM) for 2 hr. The levels of the indicated proteins in the lysates were analyzed using immunoblotting. β-actin was used as the loading control. The data shown are presentative of at least three separate experiments.

Figure 5F

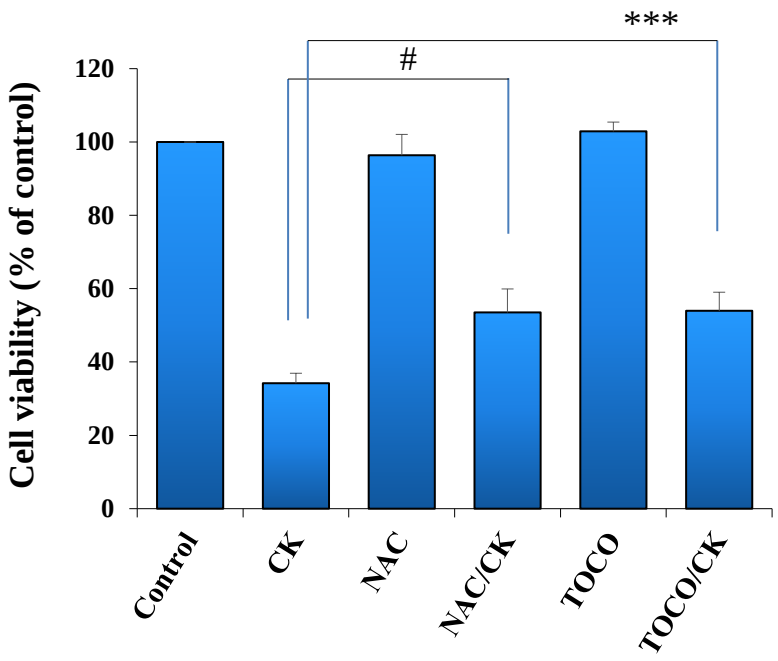

Figure 5F. H460 cells were exposed to CK (35 μg/ml) for 18 hr after pretreatment with NAC (5 mM) and tocopherol (Toco, 25 μM) for 2 hr, and their viability was determined using an MTT assay. Data are expressed as the mean ± SD of the fold-increase compared to the untreated control from three independent experiments performed in triplicate. $^{\#}P < 0.01$; $^{***}P < 0.0005$.

Figure 5G

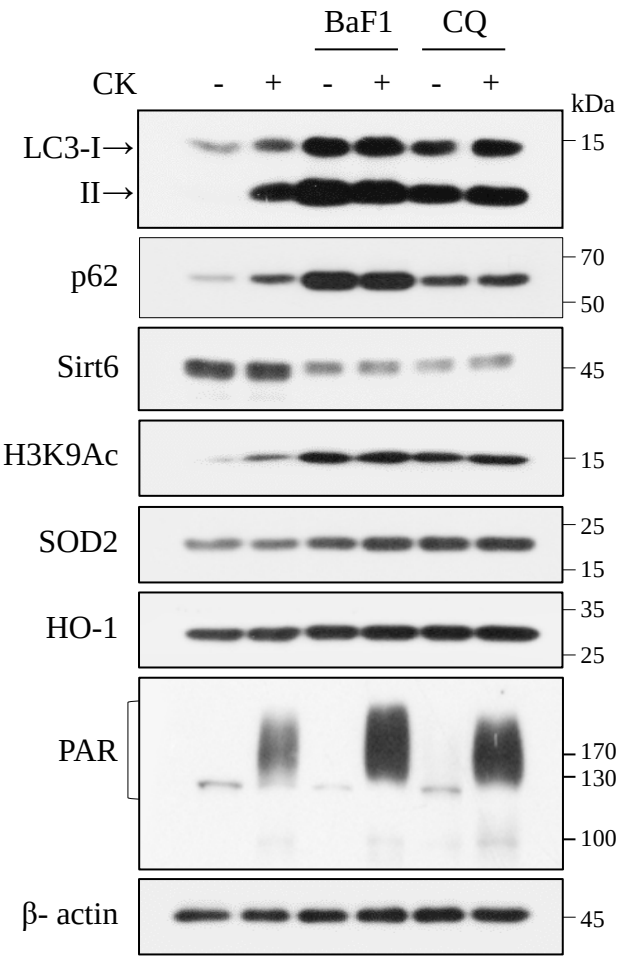

Figure 5G. Autophagy involves in inhibition of CK-induced PARP-1 activation and oxidative stress. H460 cells were exposed to CK for 18 hr with or without pretreatment with BaF1 (100 nM) and CQ (50 uM) for 2 hr. The lysates were subjected to immunoblotting for indicated proteins. β-actin was used as the loading control. The data shown are presentative of at least three separate experiments.

3.6. Subcellular localization of Sirt6 and p62 in response to CK

We found that Sirt6 protein stability was affected by oxidative stress. We next investigated how nuclear localized Sirt6 protein is reduced under oxidative stress. Our previous study showed that p62 plays a critical role in intracellular redistribution of Sirt6 in cadmium-exposed mouse kidney MES13E cells (So et al., 2021). Furthermore, p62 shuttles between the nucleus and cytosol, acting as a cargo receptor for ubiquitinated targets for degradation (Pankiv et al. 2010). Therefore, we investigated the subcellular localization of Sirt6 and p62 in the same fractionation samples as in Fig. 2D. Sirt6 was primarily localized to the nuclear-enriched insoluble fraction at the basal level and redistributed to the particulate compartment in response to CK. Moreover, at basal levels, p62 is localized to both the soluble and insoluble fractions, increasing in the soluble fraction and, to a lesser extent, in the particulate fraction after CK exposure (Fig. 6A). These results suggest the possibility for an interaction between Sirt6 and p62 proteins. To demonstrate this hypothesis, p62 gene was knocked down by transfection with p62 specific siRNA and control siRNA. CK treatment to p62-knockdowned cells, upregulated CK-induced Sirt6 protein (Fig. 6B, C). This result was further confirmed by immunofluorescence (IF) staining with anti-p62 and anti-Sirt6 antibodies. In untreated control cells, Sirt6 staining was distributed in the nucleus. After CK exposure, Sirt6 showed weak and diffuse staining in the nucleus and as punctae of various sizes in the cytoplasm. In untreated control cells, p62 was mainly localized in the perinuclear region. After CK treatment, p62 staining was observed as punctae with various size and fluorescence intensity, and the functae showed a diffuse distribution in the cytoplasm. Furthermore, p62 and Sirt6 puntae completely overlapped. Sirt6 prominantly localized in the nucleus under p62-knockdowned condition (Fig. 6D). These results therefore show that nuclear translocation of Sirt6 to the cytoplasm can be dependent on p62.

Figure 6A

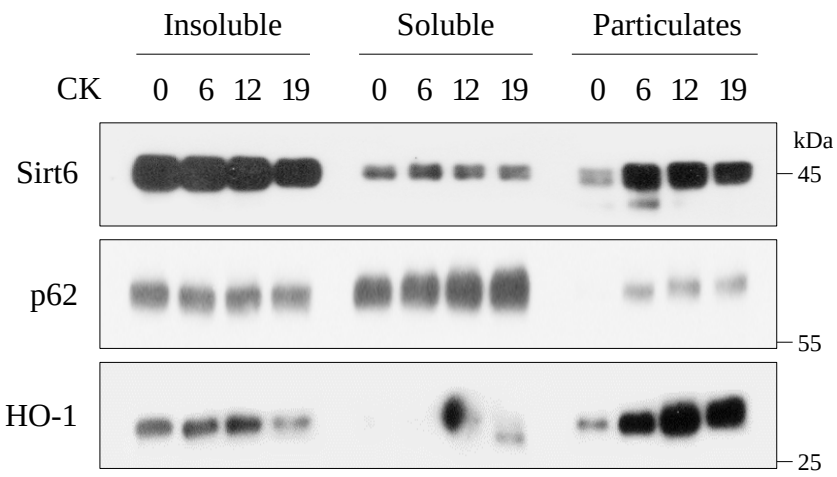

Figure 6A. Subcellular translocation of Sirt6 is p62 dependent. H460 cells were exposed to CK for 6, 12, and 19 hr and subjected to subcellular fractionation into nuclear-enriched, cytoplasmic, and mitochondria-enriched fractions. The purity of each fraction was assessed for HDAC1, β-actin, and SOD2, respectively. Determined using immunoblotting. Data are representative of n > 3.

Figure 6B-C

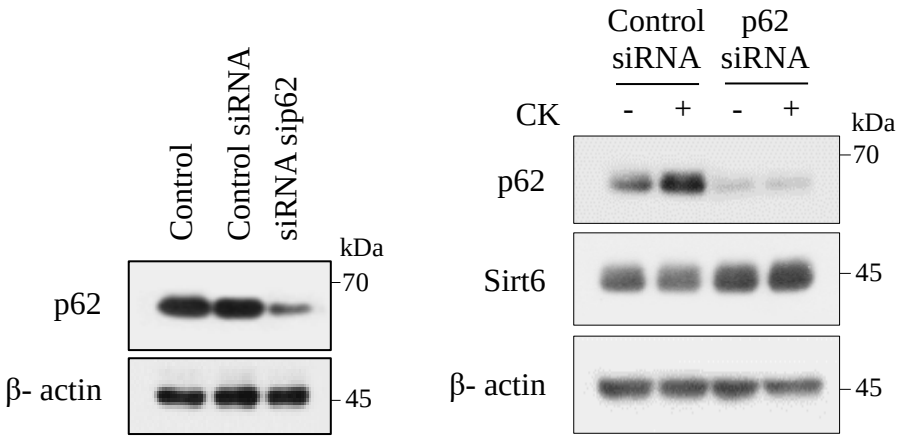

Figure 6B-C. (**B**) KD efficiency for p62-specific siRNA was evaluated by immunoblotting for p62. NC = negative control. (**C**) H460 cells were silenced with NC siRNA or p62 siRNA for overnight, and were exposed to CK (35 μg/ml) for 18 hr, and the indicated proteins were analyzed using immunoblotting. β-actin was used as the loading control (n = 3).

Figure 6D

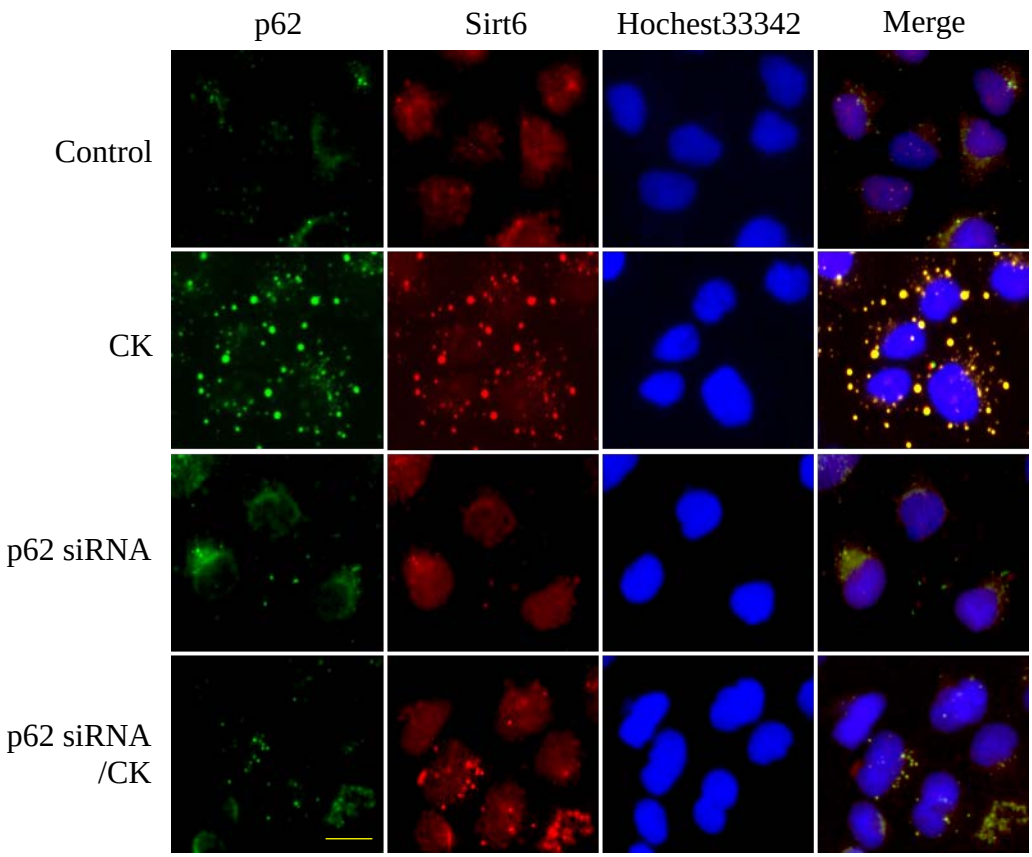

Figure 6D. Cytoplasmic translocation of Sirt6 is p62 dependent. H460 cells cultured on coverslips were silenced with NC siRNA or p62 siRNA for overnight, and treated with CK for 12 hr, fixed, and then subjected to IF staining for both Sirt6 (red) and p62 (green). Nuclei were counterstained with Hoechst 33342 (blue). Scale bar = 25 μm.

3.7. Sirt6 interacts with p62 in response to CK

To further examine the interaction between Sirt6 and p62, cells were treated with leptomysin B (LMB), a potent and specific nuclear export inhibitor. LMB treatment reduced CK-induced p62 and Sirt6 protein levels (Fig. 7A). To further elucidate these results, cells were treated with LMB and IF staining was performed for anti-p62 and anti-Sirt6 antibodies. As shown in LMB treatment significantly reduced the number of puntae and inhibited the translocation of p62 and Sirt6 to the cytoplasm, resulting in complete overlap of the two proteins in the nucleus (Fig. 7B). The possibility of the physical interactions between Sirt6 and p62 examined by co-immunoprecipitation (Co-IP). IP assays for p62 and mouse IgG were performed in lysates from CK-treated cells, followed by immunoblotting with an anti-Sirt6 antibody (Fig. 7C). Furthermore, IP analysis for ubiquitin and mouse IgG was performed with the same protein lysates, followed by immunoblotting with an anti-Sirt6 antibody (Fig. 7D). Together, these results indicate that translocation of nuclear Sirt6 to the cytoplasm is dependent on p62 and can interact with p62 through ubiquitination.

Figure 7A

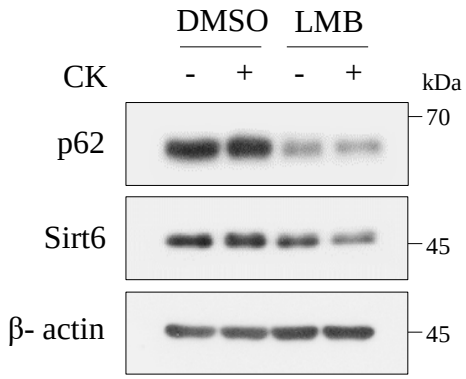

Figure 7A. Sirt6 interacts with p62 via ubiquitination. Cells were exposed to CK for 18 hr after pretreatment with LMB (25 nM) and DMSO for 2 hr, harvest, and the indicated proteins were analyzed using immunoblotting. β-actin was used as the loading control (n = 3).

Figure 7B

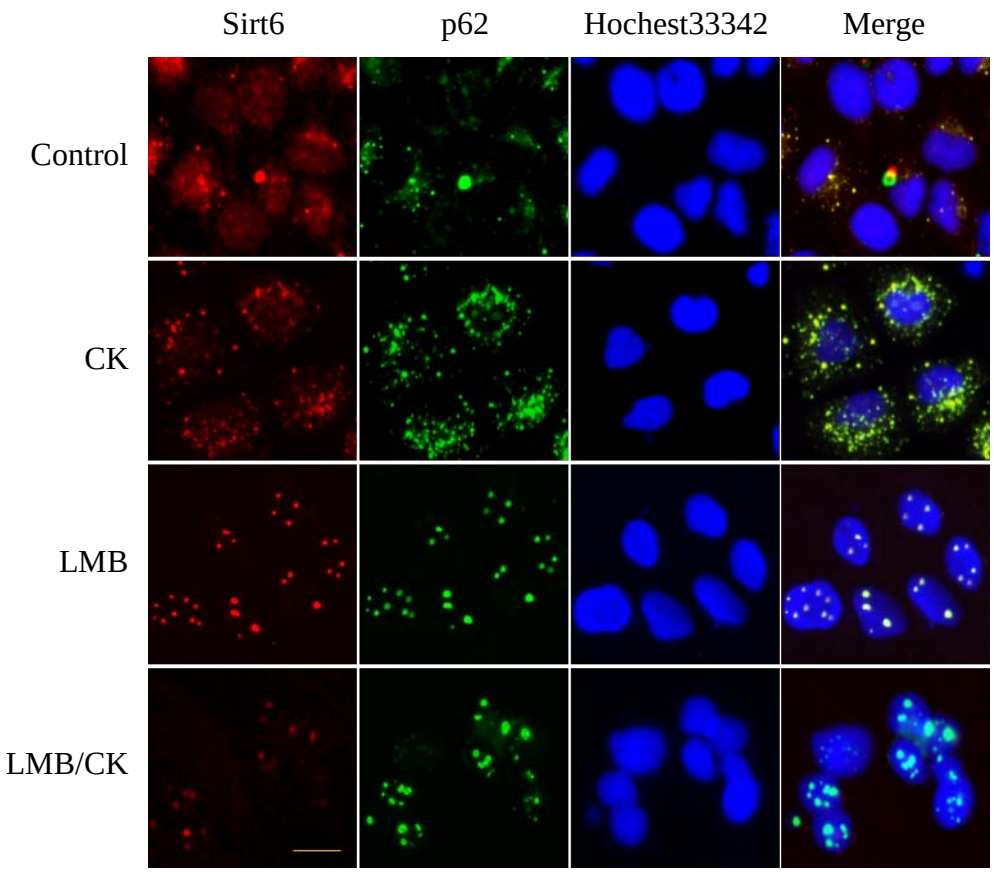

Figure 7B. Cells cultured on coverslips were exposed to CK for 12 hr after treatment with DMSO or LMB (25nM) for 2 hr, fixed, and then subjected to IF staining for both Sirt6 (red) and p62 (green). Nuclei were counterstained with Hoechst 33342 (blue). Scale bar = 25 μm.

Figure 7C-D

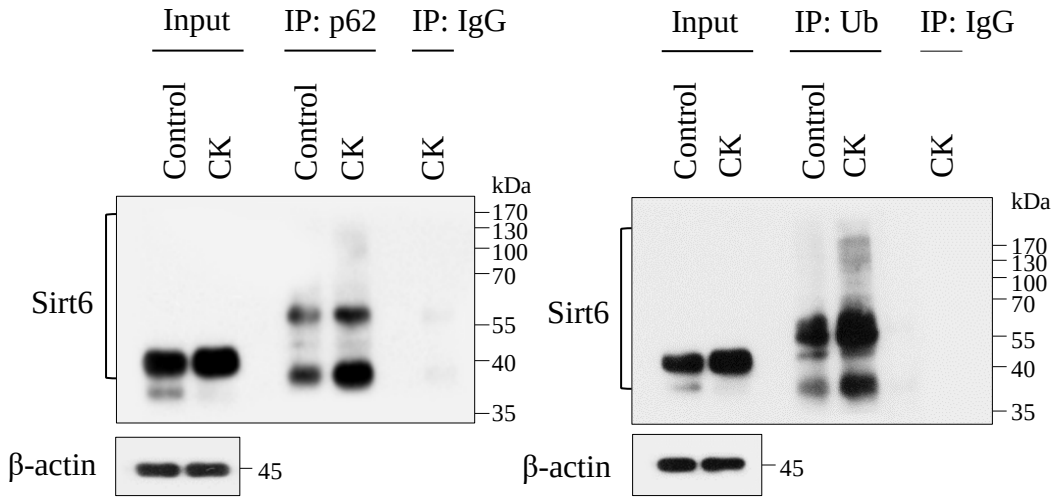

Figure 7C, D. H460 cells were exposed to CK for 12 hr. Immunoblotting was performed in lysates for Sirt6, and 800 μg of remaining protein was used for IP analysis with p62, Ub antibodies and mouse IgG, and then immunoblotted for Sirt6. Data are representative of n = 2.

4. DISCUSSION

CK has been reported to have various pharmacological effects, including anticancer property (Tom et al., 2023). In the present study, we investigated the molecular mechanisms underlying the chemopreventive effects of CK on lung cancer cells. Our study identified a new molecular mechanism induced by CK, caspase-independent PARP-1 activation mediated parthanatos, and also the role of Sirt6 in this process.

CK has been reported to have anti-cancer effects in a variety of cancer cell types, including human lung cancers, human hepatoma, and human colorectal cancers, and the effects are associated with multiple signaling pathways, cell cycle arrest, apoptosis, autophagy, and ER stress (Zhou et al., 2022; Zhang et al., 2013; Lee et al., 2010; Tam et al., 2023). Until now, many studies have been reported on the anticancer effect of CK, but the effect on lung cancer has been reported very limitedly. It has been reported that CK induced apoptosis through caspase- and mitochondrial-dependent apoptosis in lung cancer cells (HL-60, H460 cells) (Chae et al., 2009; Cho et al., 2009). CK induced ER stress through induction of ER stress markers, including GRP78/Bip, IRE1A, and eIF2A, and persistent ER stress led to ER stress-mediated apoptosis vis caspase-12 activation in A549 and SK-MES-1 human lung cancer cells (Shin et al., 2018). In addition, CK showed a synergistic effect on cisplatin-induced apoptosis in H460 and A549 cells (Li et al., 2015). Therefore, on basis of previous studies, CK-induced anti-cancer effect in lung cancers seems to be very closely related with apoptosis. In the present study, CK treatment to H460 lung cancer cells caused for cell cycle arrest through upregulating p27, p21, and p53. Although caspase-8 was reduced by CK treatment, apoptotic cleavage of caspase-3 and PARP-1 was not induced during the time of CK exposure and by the doses used. However, long-term incubation (>36 h) induced caspase-3 reduction and its downstream PARP-1 cleavage at very small, indicating that CK is not competent in canonical caspase-dependent apoptosis.

PARP are a family of proteins involved in catalyzing PARylation of its own or target proteins in a NAD+-dependent manner (Hassa et al., 2006; Kim et al., 2005). PARPs play important roles in various cellular processes, including DNA repair, genomic stability, and apoptosis, resulting

in cell survival and cell death (Morales et al., 2014). Activated PARP-1 catalyzes DNA repair process via activating multiple DNA repair -related enzymes, including DNA ligase. However, hyperactivation of PARP-1 induces parthanatos through cytoplasmic accumulation of PAR (Fatokun et al., 2014). Thus, PARP-1 activation not only promotes cell survival but can also act as an inducer of cell death. In addition, upon massive DNA damage, PARP-1 is cleaved by caspases 3 and 7, to two enzymatically inactive fragments (89 and 24 kDa) and inducing apoptosis (D'Amours et al., 2001). Parthanatos is a caspase-independent and PARP-1 overactivation-mediated cell death and involeves in various pathophysiology, including tumor, neuronal diseases, and cardiovascular diseases (Liu et al., 2022). The characteristics of parthanatos are PARP-1 hyperactivation, AIF nuclear translocation, large-scale DNA fragmentation and chromatin condensation distinct from apoptotic nuclear fragmentation, and mitochondrial membrane depolarization (Huang et al., 2022; Fatokun et al., 2014). In the present study, we found that CK treatment induced nuclear morphological characteristics of parthanatos, and induced hyperactivation of PARP-1, translocation of PAR to the cytoplasm and nuclear translocation of AIF. Inactivation of CK-induced PARP-1 using PARP-1 inhibitors such as 3-AB or ANI induces apoptotic PARP-1 cleavage, suggesting that CK can induce a cell death mode in a context-dependent manner. However, what causes PARP-1 overactivation is not clear. We confirmed that PARylation by CK was inhibited by PARP-1 inhibitors and exogenous NAD+, but was affected to a very low level by antioxidants and inhibition of autophagy and the proteasome. This indicates that PARP-1 activation may be related to intracellular NAD+ and ATP levels.

Mammalian sirtuins (Sirt1-7) function as deacetylases or mono-ADP-ribosyl-transferases. Sirtuin family members have different subcellular localization and different functions (Santos et al. 2013). Sirt6 is predominantly nuclear-localized protein and functions as both mono-ADP-ribosyl transferase and NAD^+-dependent deacetylase (Liszt et al. 2005). Therefore, changes in subcellular localization and protein expression level may be critical factors for the function of Sirt6 (Morigi et al. 2018; Wang et al. 2019). Sirt6 plays a critical role as a metabolic sensor

against a various stress. Sirt6 protein stability is regulated at transcriptional level through p53 (Kanfi et al., 2008) and c-Jun/c-Fos pathway (Min et al., 2012). It is also regulated by post-transcriptional modifications. Proteasome inhibition through noncanonical ubiquitination by the ubiquitin ligase C-terminus of Hsp70 interacting protein (CHIP) or deubiquitination by ubiquitin-specific peptidase (USP10) plays an important role in Sirt6 stability (Lin et al. 2013; Ronnebaum et al. 2013), suggesting that ubiquitin-proteasome pathway plays a critical role in Sirt6 protein stability. Indeed, we demonstrated the interaction between ubiquitin and Sirt6 through co-IP. However, proteasome inhibition by MG132 did not upregulate but rather further reduced CK-induced reduced Sirt6 levels (data not shown), indicating that ubiquitinated Sirt6 is not a proteasome target. In addition, autophagy inhibition through chemical inhibitors showed similar results to proteasome inhibition. We found that Sirt6 protein was upregulated by antioxidants such as NAC and tocopherol, indicating that Sirt6 stability is regulated by oxidative stress. When autophagy or proteasome were inhibited, HO-1 and SOD2 upregulated, resulting in Sirt6 decreasing and increasing PARylation level. Therefore, based on these results, the CK-induced Sirt6 protein reduction after autophagy or proteasome inhibition may be related to oxidative stress. Indeed, inhibition of autophagy, HO-1 and SOD_2 levels increased in response to CK. In addition, CK-induced HO-1 is increased by Sirt6 knockdown and decreased by Sirt6 overexpression. It has been reported that sirtuins, including Sirt2, Sirt6, and Sit7, modulates oxidative stress genes and related signaling pathways (Singh et al., 2018). It has also been reported that Sirt6 plays a protective role via regulating NRF2-HO-1 antioxidant pathway in response to oxidative stress (Mao et al., 2011; Pan et al., 2016). Therefore, Sirt6 not only protected ischemia/reperfusion injury against oxidative stress through regulating antioxidants (Wang et al., 2016), but also protected human mesenchymal stem cells (hMSCs) from oxidative stress through activation of NRF2 (Pan et al., 2016). Whereas, Sirt6 induces apoptosis and mitochondrial dysfunction via promoting ROS production in many cell types (Yu et al., 2019). In this study, we found that CK treatment reduced Sirt6 protein and induced antioxidants such as HO-1 and SOD2, which were rescued by NAC treatment or Sirt6 overexpression. These results

suggest that an important factor in CK-induced cell death may be oxidative stress due to reduced Sirt6 protein levels. As further evidence for our hypothesis, Sirt6 protein is reduced through inhibition of autophagy and proteasome, upregulating antioxidant enzymes including HO-1 and SOD2 and further reducing cell viability compared to CK-treated cells.

MonoADP- ribosylation of Sirt6 has been reported to play an important role in activating the NRF2 target HO-1 (Rezazadeh et al., 2019), indicating that Sirt6 is required for HO-1 induction under oxidative stress. However, our study showed that Sirt6 reduction caused for induction of oxidative stress, therebying increasing the antioxidant enzymes HO-1 and SOD2. Moreover, Sirt6 was observed to translocate into the particulate fraction after CK treatment, suggesting that Sirt6 plays a role in the cytosol rather than the nucleus. Therefore, to better understand Sirt6 function, it is necessary to find Sirt6 target organelles.

Given that the functions of sirtuins can depend on their subcellular localization (Michishita et al. 2005; Santos et al. 2013). In the present study, we found that Sirt6 translocated from nuclear rich fractions to particulate fractions after CK treatment, which was inhibited by LMB treatment. However, it is unclear how nuclear localized Sirt6 translocates to cytoplasmic compartments in response to CK. In this context, we thought that Sirt6 translocation may be dependent on p62, showing increasing level in response to CK. p62 is a multifunctional protein that contains various protein –protein interaction domains, including and N-terminal PB1, a nuclear localization signal (NLS), an export signal (NES), the LC3-interacting region (LIR), and a C-terminal Ub-associated domain (UBA), indicating that p62 involves in the regulation of diverse cellular signaling including oxidative stress signaling and homeostasis of multiple proteins (Moscat and Diaz-Meco, 2009). p62 activates transcription factor NF-E2-related factor 2 (NRF2)- HO-1 signaling pathway through direct interaction with the ubiquitin ligase Kelch-like ECH-associated protein 1 (KEAP1) (Kobayashi et al., 2004). p62 also regulates intracellular protein quality control by targeting ubiquitinated substrates and recruiting them to the autophagosome or proteasome for degradation (Pankiv et al. 2010). Furthermore, p62 involves in nuclear quality control via NLS and NES (Moscat and Diaz-Meco 2009). CK treatment led to subcellular redistribution of p62

and Sirt6 to predominantly soluble and particulates compartments, respectively. Consistently, IF staining showed that p62 and Sirt6 were detected as various sizes of punctae in the cytoplasm after CK treatment and merged, indicating that intracellular redistribution of Sirt6 might be dependent of p62 for degradation. Co-IP experiments showed that Sirt6 interacted with ubiquitin and p62, suggesting that Sirt6 can interact with p62 via ubiquitination. Together, p62 might be involves in subcellular redistribution of Sirt6. Although we have demonstrated intracellular translocation of Sirt6 primarily to the particulate fraction, it is unclear where Sirt6 is located. We believe that elucidating the target organelles of Sirt6 is of great importance for understanding Sirt6 function.

In conclusion, the present study demonstrated that the novel molecular mechanism of CK -induced chemopreventive effect in lung cancer cells. CK induced PARP-1 hyperactivation-mediated parthanatos, facilitating by oxidative stress-mediated Sirt6 reduction.

5. REFERENCES

1. Liszt G, Ford E, Kurtev M, Guarente L. Mouse Sir2 Homolog SIRT6 is a Nuclear ADP-Ribosyltransferase. J Biol Chem. 280:21313–20. 2005.
2. Sharma A, Mahur P, Muthukumaran J, Singh AK, Jain M. Shedding light on structure, function and regulation of human sirtuins: a comprehensive review. 3 Biotech. 13:29. 2023.
3. Mostoslavsky R, Chua KF, Lombard DB, Pang WW, Fischer MR, Gellon L, Liu P, Mostoslavsky G, Franco S, Murphy MM, Mills KD, Patel P, Hsu JT, Hong AL, Ford E, Cheng HL, Kennedy C, Nunez N, Bronson R, Frendewey D, Auerbach W, Valenzuela D, Karow M, Hottiger MO, Hursting S, Barrett JC, Guarente L, Mulligan R, Demple B, Yancopoulos GD, Alt FW. Genomic instability and aging-like phenotype in the absence of mammalian SIRT6. Cell. 124:315-29. 2006.
4. Houtkooper RH, Pirinen E, Auwerx J: Sirtuins as regulators of metabolism and healthspan. Nat Rev Mol Cell Biol. 13:225–238. 2012.
5. Campos-Melo D, Hawley ZCE, Droppelmann CA, Strong MJ. The Integral Role of RNA in Stress Granule Formation and Function. Front Cell Dev Biol. 9:621-779. 2021.
6. Jedrusik-Bode M, Studencka M, Smolka C, Baumann T, Schmidt H, Kampf J, Paap F, Martin S, Tazi J, Müller KM, Krüger M, Braun T, Bober E. The sirtuin SIRT6 regulates stress granule formation in C. elegans and mammals. J Cell Sci. 126:5166-77. 2013.
7. Jiang H, Khan S, Wang Y, Charron G, He B, Sebastian C, Du J, Kim R, Ge E, Mostoslavsky R, Hang HC, Hao Q, Lin H. SIRT6 regulates TNF-α secretion through hydrolysis of long-chain fatty acyl lysine. Nature. 496:110-3. 2013.
8. Bresque M, Cal K, Pérez-Torrado V, Colman L, Rodríguez-Duarte J, Vilaseca C, Santos L, Garat MP, Ruiz S, Evans F, Dapueto R, Contreras P, Calliari A, Escande C. SIRT6 stabilization and cytoplasmic localization in macrophages regulates acute and chronic inflammation in mice. J Biol Chem. 298:101711. 2022.
9. Marquardt JU, Fischer K, Baus K, Kashyap A, Ma S, Krupp M, Linke M, Teufel A, Zechner

U, Strand D, Thorgeirsson SS, Galle PR, Strand S. Sirtuin-6-dependent genetic and epigenetic alterations are associated with poor clinical outcome in hepatocellular carcinoma patients. Hepatology. 58:1054-64. 2013.

10. Liu W, Wu M, Du H, Shi X, Zhang T and Li J: SIRT6 inhibits colorectal cancer stem cell proliferation by targeting CDC25A. Oncol Lett. 15: 5368-5374. 2018
11. Baeken MW, Schwarz M, Kern A, Moosmann B, Hajieva P, Behl C. The selective degradation of sirtuins via macroautophagy in the MPP^+ model of Parkinson's disease is promoted by conserved oxidation sites. Cell Death Discov. 7:286. 2021.
12. Khongkow M, Olmos Y, Gong C, Gomes AR, Monteiro LJ, Yagüe E, Cavaco TB, Khongkow P, Man EP, Laohasinnarong S, Koo CY, Harada-Shoji N, Tsang JW, Coombes RC, Schwer B, Khoo US, Lam EW. SIRT6 modulates paclitaxel and epirubicin resistance and survival in breast cancer. Carcinogenesis. 34:1476-86. 2013.
13. Liu Y, Xie QR, Wang B, Shao J, Zhang T, Liu T, Huang G, Xia W. Inhibition of SIRT6 in prostate cancer reduces cell viability and increases sensitivity to chemotherapeutics. Protein Cell. 4:702-10. 2013.
14. Krishnamoorthy V, Vilwanathan R. Silencing Sirtuin 6 induces cell cycle arrest and apoptosis in non-small cell lung cancer cell lines. Genomics. 112:3703-3712. 2020
15. Morales J, Li L, Fattah FJ, Dong Y, Bey EA, Patel M, Gao J, Boothman DA. Review of poly (ADP-ribose) polymerase (PARP) mechanisms of action and rationale for targeting in cancer and other diseases. Crit Rev Eukaryot Gene Expr. 24:15-28. 2014.
16. Luo X, Kraus WL. On PAR with PARP: cellular stress signaling through poly(ADP-ribose) and PARP-1. Genes Dev. 26:417-32. 2012.
17. Andrabi SA, Kim NS, Yu SW, Wang H, Koh DW, Sasaki M, Klaus JA, Otsuka T, Zhang Z, Koehler RC, Hurn PD, Poirier GG, Dawson VL, Dawson TM. Poly(ADP-ribose) (PAR) polymer is a death signal. Proc Natl Acad Sci U S A. 103:18308-13. 2006.
18. D'Amours D, Sallmann FR, Dixit VM, Poirier GG. Gain-of-function of poly(ADP-ribose) polymerase-1 upon cleavage by apoptotic proteases: implications for apoptosis. J Cell Sci.

114:3771-8. 2001.

19. Van Meter M, Mao Z, Gorbunova V, Seluanov A. Repairing split ends: SIRT6, mono-ADP ribosylation and DNA repair. Aging (Albany NY). 3:829-35. 2011.
20. Tam DNH, Nam NH, Cuong NTK, Hung DT, Soa DT, Altom A, Tran L, Elhadad H, Huy NT. Compound K: A systematic review of its anticancer properties and probable mechanisms. Fundam Clin Pharmacol. 37:684-712. 2023.
21. Zhang X, Zhang S, Sun Q, Jiao W, Yan Y, Zhang X. Compound K Induces Endoplasmic Reticulum Stress and Apoptosis in Human Liver Cancer Cells by Regulating STAT3. Molecules. 23:1482. 2018.
22. Shin DH, Leem DG, Shin JS, Kim JI, Kim KT, Choi SY, Lee MH, Choi JH, Lee KT. Compound K induced apoptosis via endoplasmic reticulum Ca^{2+} release through ryanodine receptor in human lung cancer cells. J Ginseng Res. 42:165-174. 2018.
23. Lee IK, Kang KA, Lim CM, Kim KC, Kim HS, Kim DH, Kim BJ, Chang WY, Choi JH, Hyun JW. Compound K, a metabolite of ginseng saponin, induces mitochondria-dependent and caspase-dependent apoptosis via the generation of reactive oxygen species in human colon cancer cells. Int J Mol Sci. 11:4916-31. 2010.
24. Li C, Dong Y, Wang L, Xu G, Yang Q, Tang X, Qiao Y, Cong Z. Ginsenoside metabolite compound K induces apoptosis and autophagy in non-small cell lung cancer cells via AMPK-mTOR and JNK pathways. Biochem Cell Biol. 97:406-414. 2019.
25. Yang Z, Yu Y, Sun N, Zhou L, Zhang D, Chen H, Miao W, Gao W, Zhang C, Liu C, Yang X, Wu X, Gao Y. Ginsenosides Rc, as a novel SIRT6 activator, protects mice against high fat diet induced NAFLD. J Ginseng Res. 47:376-384. 2023.
26. Oh H, Cho W, Park SY, Abd El-Aty AM, Jeong JH, Jung TW. Ginsenoside Rb3 ameliorates podocyte injury under hyperlipidemic conditions *via* PPARδ- or SIRT6-mediated suppression of inflammation and oxidative stress. J Ginseng Res. 47:400-407. 2023.
27. Azuma Y, Yokobori T, Mogi A, Altan B, Yajima T, Kosaka T, Onozato R, Yamaki E, Asao T, Nishiyama M, Kuwano H. SIRT6 expression is associated with poor prognosis and

chemosensitivity in patients with non-small cell lung cancer. J Surg Oncol. 112:231-7. 2015.

28. Choi JE, Mostoslavsky R. Sirtuins, metabolism, and DNA repair. Curr Opin Genet Dev. 26:24-32. 2014.
29. Mao Z, Hine C, Tian X, Van Meter M, Au M, Vaidya A, Seluanov A, Gorbunova V. SIRT6 promotes DNA repair under stress by activating PARP1. Science. 332:1443-6. 2011.
30. Loesberg C, van Rooij H, Smets LA. Meta-iodobenzylguanidine (MIBG), a novel high-affinity substrate for cholera toxin that interferes with cellular mono(ADP-ribosylation). Biochim Biophys Acta. 1037:92-9. 1990.
31. Liu L, Su X, Quinn WJ 3rd, Hui S, Krukenberg K, Frederick DW, Redpath P, Zhan L, Chellappa K, White E, Migaud M, Mitchison TJ, Baur JA, Rabinowitz JD. Quantitative Analysis of NAD Synthesis-Breakdown Fluxes. Cell Metab. 27:1067-1080. 2018.
32. Pan H, Guan D, Liu X, Li J, Wang L, Wu J, Zhou J, Zhang W, Ren R, Zhang W, Li Y, Yang J, Hao Y, Yuan T, Yuan G, Wang H, Ju Z, Mao Z, Li J, Qu J, Tang F, Liu GH. SIRT6 safeguards human mesenchymal stem cells from oxidative stress by coactivating NRF2. Cell Res. 26:190-205. 2016.
33. So KY, Park BH, Oh SH. Cytoplasmic sirtuin 6 translocation mediated by p62 polyubiquitination plays a critical role in cadmium-induced kidney toxicity. Cell Biol Toxicol. 37:193-207. 2021.
34. Ichimura Y, Kominami E, Tanaka K, Komatsu M. Selective turnover of p62/A170/SQSTM1 by autophagy. Autophagy. 4:1063-6. 2008.
35. Pankiv S, Lamark T, Bruun JA, Øvervatn A, Bjørkøy G, Johansen T. Nucleocytoplasmic shuttling of p62/SQSTM1 and its role in recruitment of nuclear polyubiquitinated proteins to promyelocytic leukemia bodies. J Biol Chem. 285:5941-53. 2010.
36. Zhou L, Li ZK, Li CY, Liang YQ, Yang F. Anticancer properties and pharmaceutical applications of ginsenoside compound K: A review. Chem Biol Drug Des. 99:286-300. 2022.
37. Zhang Z, Du GJ, Wang CZ, Wen XD, Calway T, Li Z, He TC, Du W, Bissonnette M, Musch MW, Chang EB, Yuan CS. Compound K, a Ginsenoside Metabolite, Inhibits Colon Cancer

Growth via Multiple Pathways Including p53-p21 Interactions. Int J Mol Sci. 14:2980-95. 2013.

38. Lee IK, Kang KA, Lim CM, Kim KC, Kim HS, Kim DH, Kim BJ, Chang WY, Choi JH, Hyun JW. Compound K, a metabolite of ginseng saponin, induces mitochondria-dependent and caspase-dependent apoptosis via the generation of reactive oxygen species in human colon cancer cells. Int J Mol Sci. 11:4916-31. 2010.
39. Tam DNH, Nam NH, Cuong NTK, Hung DT, Soa DT, Altom A, Tran L, Elhadad H, Huy NT. Compound K: A systematic review of its anticancer properties and probable mechanisms. Fundam Clin Pharmacol. 37:684-712. 2023.
40. Chae S, Kang KA, Chang WY, Kim MJ, Lee SJ, Lee YS, Kim HS, Kim DH, Hyun JW. Effect of compound K, a metabolite of ginseng saponin, combined with gamma-ray radiation in human lung cancer cells in vitro and in vivo. J Agric Food Chem. 57:5777-82. 2009.
41. Cho SH, Chung KS, Choi JH, Kim DH, Lee KT. Compound K, a metabolite of ginseng saponin, induces apoptosis via caspase-8-dependent pathway in HL-60 human leukemia cells. BMC Cancer. 9:449. 2009.
42. Li Y, Zhou T, Ma C, Song W, Zhang J, Yu Z. Ginsenoside metabolite compound K enhances the efficacy of cisplatin in lung cancer cells. J Thorac Dis. 7:400-6. 2015.
43. Hassa PO, Haenni SS, Elser M, Hottiger MO. Nuclear ADP-ribosylation reactions in mammalian cells: where are we today and where are we going? Microbiol Mol Biol Rev. 70:789-829. 2006.
44. Kim MY, Zhang T, Kraus WL. Poly(ADP-ribosyl)ation by PARP-1: 'PAR-laying' NAD+ into a nuclear signal. Genes Dev. 19:1951-67. 2005.
45. Morales J, Li L, Fattah FJ, Dong Y, Bey EA, Patel M, Gao J, Boothman DA. Review of poly (ADP-ribose) polymerase (PARP) mechanisms of action and rationale for targeting in cancer and other diseases. Crit Rev Eukaryot Gene Expr. 24:15-28. 2014.
46. Fatokun AA, Dawson VL, Dawson TM. Parthanatos: mitochondrial-linked mechanisms and therapeutic opportunities. Br J Pharmacol. 171:2000-16. 2014.

47. D'Amours D, Sallmann FR, Dixit VM, Poirier GG. Gain-of-function of poly(ADP-ribose) polymerase-1 upon cleavage by apoptotic proteases: implications for apoptosis. J Cell Sci. 114:3771-8. 2001.
48. Liu S, Luo W, Wang Y. Emerging role of PARP-1 and PARthanatos in ischemic stroke. J Neurochem. 160:74-87. 2022.
49. Huang P, Chen G, Jin W, Mao K, Wan H, He Y. Molecular Mechanisms of Parthanatos and Its Role in Diverse Diseases. Int J Mol Sci. 23:7292. 2022.
50. Fatokun AA, Dawson VL, Dawson TM. Parthanatos: mitochondrial-linked mechanisms and therapeutic opportunities. Br J Pharmacol. 171:2000-16. 2014.
51. Houtkooper RH, Pirinen E, Auwerx J. Sirtuins as regulators of metabolism and healthspan. Nat Rev Mol Cell Biol. 13:225-238. 2012.
52. Morigi M, Perico L, Benigni A. Sirtuins in Renal Health and Disease. J Am Soc Nephrol. 29:1799-1809. 2018.
53. Wang T, Sun C, Hu L, Gao E, Li C, Wang H, Sun D. Sirt6 stabilizes atherosclerosis plaques by promoting macrophage autophagy and reducing contact with endothelial cells. Biochem Cell Biol. 98:120-129. 2020.
54. Kanfi Y, Shalman R, Peshti V, Pilosof SN, Gozlan YM, Pearson KJ, Lerrer B, Moazed D, Marine JC, de Cabo R, Cohen HY. Regulation of SIRT6 protein levels by nutrient availability. FEBS Lett. 582:543-8. 2008.
55. Min L, Ji Y, Bakiri L, et al. Liver cancer initiation is controlled by AP-1 through SIRT6-dependent inhibition of survivin. *Nat Cell Biol*. 14:1203–1211. 2012.
56. Lin Z, Yang H, Tan C, Li J, Liu Z, Quan Q, Kong S, Ye J, Gao B, Fang D. USP10 antagonizes c-Myc transcriptional activation through SIRT6 stabilization to suppress tumor formation. Cell Rep. 5:1639-49. 2013.
57. Ronnebaum SM, Wu Y, McDonough H, Patterson C. The ubiquitin ligase CHIP prevents SirT6 degradation through noncanonical ubiquitination. Mol Cell Biol. 33:4461-72. 2013.
58. Singh CK, Chhabra G, Ndiaye MA, Garcia-Peterson LM, Mack NJ, Ahmad N. The Role of

Sirtuins in Antioxidant and Redox Signaling. Antioxid Redox Signal. 28:643-661. 2018.

59. Mao Z, Hine C, Tian X, Van Meter M, Au M, Vaidya A, Seluanov A, Gorbunova V. SIRT6 promotes DNA repair under stress by activating PARP1. Science. 332:1443-6. 2011.
60. Wang XX, Wang XL, Tong MM, Gan L, Chen H, Wu SS, Chen JX, Li RL, Wu Y, Zhang HY, Zhu Y, Li YX, He JH, Wang M, Jiang W. SIRT6 protects cardiomyocytes against ischemia/reperfusion injury by augmenting FoxO3α-dependent antioxidant defense mechanisms. Basic. Res. Cardiol. 111:13. 2016.
61. Yu W, Yang Z, Huang R, Min Z, Ye M. SIRT6 promotes the Warburg effect of papillary thyroid cancer cell BCPAP through reactive oxygen species. Onco Targets Ther. 12:2861-2868. 2019.
62. Rezazadeh S, Yang D, Tombline G, Simon M, Regan SP, Seluanov A, Gorbunova V. SIRT6 promotes transcription of a subset of NRF2 targets by mono-ADP-ribosylating BAF170. Nucleic Acids Res. 47:7914-7928. 2019.
63. Michishita E, Park JY, Burneskis JM, Barrett JC, Horikawa I. Evolutionarily conserved and nonconserved cellular localizations and functions of human SIRT proteins. Mol Biol Cell. 16:4623-35. 2005.
64. Moscat J, Diaz-Meco MT. p62 at the crossroads of autophagy, apoptosis, and cancer. Cell. 137:1001-4. 2009.
65. Kobayashi A, Kang MI, Okawa H, Ohtsuji M, Zenke Y, Chiba T, Igarashi K, and Yamamoto M. Oxidative stress sensor Keap1 functions as an adaptor for Cul3-based E3 ligase to regulate proteasomal degradation of Nrf2. Mol Cell Biol. 24:7130–7139. 2004.
66. Pankiv S, Lamark T, Bruun JA, Øvervatn A, Bjørkøy G, Johansen T. Nucleocytoplasmic shuttling of p62/SQSTM1 and its role in recruitment of nuclear polyubiquitinated proteins to promyelocytic leukemia bodies. J Biol Chem. 285:5941-53. 2010.